DOE/NASA/0352-2
NASA CR-179475
DEN3-352

Sliding Seal Materials For Adiabatic Engines Phase II Interim Report

(NASA-CR-179475) SLIDING SEAL MATERIALS FOR ADIABATIC ENGINES, PHASE 2 Interim Report, Feb. 1985 - Feb. 1986 (Southwest Research Inst.) 54 p CSCL 11B G3/27

N86-29042
Unclas
43482

James Lankford and William Wei
Southwest Research Institute
San Antonio, Texas

April 1986

Prepared for
NATIONAL AERONAUTICS AND SPACE ADMINISTRATION
Lewis Research Center
Under Contract DEN3-352

for
U.S. DEPARTMENT OF ENERGY
Conservation and Renewable Energy
Office of Vehicle and Engine R&D

DOE/NASA/0352-2
NASA CR-179475
DEN3-352

Sliding Seal Materials For Adiabatic Engines Phase II Interim Report

James Lankford and William Wei
Southwest Research Institute
San Antonio, Texas

April 1986

Prepared for
NATIONAL AERONAUTICS AND SPACE ADMINISTRATION
Lewis Research Center
Under Contract DEN3-352

for
U.S. DEPARTMENT OF ENERGY
Conservation and Renewable Energy
Office of Vehicle and Engine R&D

DOE/NASA/0352-2
NASA CR-179475
DEN3-352

Sliding Seal Materials For Adiabatic Engines Phase II Interim Report

James Lankford and William Wei
Southwest Research Institute
San Antonio, Texas

April 1986

Prepared for
National Aeronautics and Space Administration
Lewis Research Center
Cleveland, Ohio 44135
Under Contract DEN3-352

for
U.S. DEPARTMENT OF ENERGY
Conservation and Renewable Energy
Office of Vehicle and Engine R&D
Washington, D.C. 20545
Under Interagency Agreement DE-A101-86CE50162

DOE/NASA/0352-2
NASA CR-179475
DEN3-352

Sliding Seal Materials For Adiabatic Engines Phase II Interim Report

James Lankford and William Wei
Southwest Research Institute
San Antonio, Texas

April 1986

Prepared for
National Aeronautics and Space Administration
Lewis Research Center
Cleveland, Ohio 44135
Under Contract DEN3-352

for
U.S. DEPARTMENT OF ENERGY
Conservation and Renewable Energy
Office of Vehicle and Engine R&D
Washington, D.C. 20545
Under Interagency Agreement DE-A101-86CE50162

1. Report No.	2. Government Accession No.	3. Recipient's Catalog No.
NASA CR-179475		

4. Title and Subtitle	5. Report Date
Sliding Seal Materials for Adiabatic Engines	April 1986
	6. Performing Organization Code

7. Author(s)	8. Performing Organization Report No.
James Lankford William Wei	06-7963 Feb. 1985 - Feb. 1986
	10. Work Unit No.

9. Performing Organization Name and Address	11. Contract or Grant No.
Southwest Research Institute 6220 Culebra Road, P. O. Drawer 28510 San Antonio, Texas 78284	DEN3-352
	13. Type of Report and Period Covered Interim Contractor Report
12. Sponsoring Agency Name and Address U.S. Department of Energy Office of Vehicle and Engine R&D Washington, D.C. 20545	14. Sponsoring Agency Code DOE/NASA/0352-2

15. Supplementary Notes

Phase II Interim Report. Prepared under Interagency Agreement DE-AI01-86CE-50162. Project Manager, Howard G. Yacobucci, Propulsion Systems Division, NASA Lewis Research Center, Cleveland, Ohio 44135.

16. Abstract

An essential task in the development of the heavy duty adiabatic diesel engine is identification and improvements of reliable, low-friction piston seal materials. In the present study, the sliding friction coefficients and wear rates of promising carbide, oxide, and nitride materials were measured under temperature, environmental, velocity, and loading conditions that are representative of the adiabatic engine environment. In addition, silicon nitride and partially stabilized zirconia disks were ion implanted with TiNi, Ni, Co, and Cr, and subsequently run against carbide pins, with the objective of producing reduced friction via solid lubrication at elevated temperature.

In order to provide guidance needed to improve materials for this application, the program stressed fundamental understanding of the mechanisms involved in friction and wear. Electron microscopy was used to elucidate the micromechanisms of wear following wear testing, and Auger electron spectroscopy was used to evaluate interface/environment interactions which seemed to be important in the friction and wear process.

Unmodified ceramic sliding couples were characterized at all temperatures by friction coefficients of 0.24 and above. The coefficient at 800°C in an oxidizing environment was reduced to below 0.1, for certain material combinations, by the ion implantation of TiNi or Co. This beneficial effect was found to derive from lubricious Ti, Ni, and Co oxides.

17. Key Words (Suggested by Author(s))	18. Distribution Statement
Ceramics; friction; wear; temperature effects; environmental effects; ion implantation; solid lubrication	Unclassified-Unlimited

19. Security Classif. (of this report)	20. Security Classif. (of this page)	21. No. of pages	22. Price*
Unclassified	Unclassified	46 + Prelim.	

*For sale by the National Technical Information Service, Springfield, Virginia 22161

ABSTRACT

An essential task in the development of the heavy-duty adiabatic diesel engine is identification and improvements of reliable, low-friction piston seal materials. In the present study, the sliding friction coefficients and wear rates of promising carbide, oxide, and nitride materials were measured under temperature, environmental, velocity, and loading conditions that are representative of the adiabatic engine environment. In addition, silicon nitride and partially stabilized zirconia disks were ion implanted with TiNi, Ni, Co, and Cr, and subsequently run against carbide pins, with the objective of producing reduced friction via solid lubrication at elevated temperature.

In order to provide guidance needed to improve materials for this application, the program stressed fundamental understanding of the mechanisms involved in friction and wear. Electron microscopy was used to elucidate the micromechanisms of wear following wear testing, and Auger electron spectroscopy was used to evaluate interface/environment interactions which seemed to be important in the friction and wear process.

Unmodified ceramic sliding couples were characterized at all temperatures by friction coefficients of 0.24 and above. The coefficient at 800 C in an oxidizing environment was reduced to below 0.1, for certain material combinations, by the ion implantation of TiNi or Co. This beneficial effect was found to derive from lubricious Ti, Ni, and Co oxides.

The present report describes in detail the results of the second year (Phase II) of a projected three-year program. The first year (Phase I) was aimed at establishing the friction and wear behavior of simple ceramic couples, and this work is summarized briefly in the Introduction.

TABLE OF CONTENTS

LIST OF ILLUSTRATIONS

LIST OF ILLUSTRATIONS (CONTINUED)

I. FRICTION AND WEAR TESTING

A. Introduction

Improvements in low heat rejection engines require components to endure contact at temperatures considerably in excess of those attainable by current metal alloys. The obvious candidate materials for fulfilling these needs are ceramics, but only as part of an integrated ceramic/lubricant system, since conventional liquid lubricants break down at temperatures above a few hundred degrees Centigrade. The objective of this report is to describe the results of a study aimed at establishing the feasibility of high-temperature, self-lubricating metal ion-implanted ceramics.

In the last few years, numerous investigators have explored the friction and wear of ceramic-ceramic couples (1-3). Although couples exhibiting minimum wear can be identified, wear is never negligible, and the unlubricated sliding friction coefficient is usually discouragingly high, i.e., $\mu_F \gtrsim 0.2$ (1-9). It has generally been concluded that ceramic components will not be used unlubricated in sliding contact engine applications at either low (1) or elevated (2) temperatures.

While this is a discouraging conclusion, especially in light of the breakdown of conventional lubricants at elevated temperature, certain other related work suggests alternative approaches to the problem. In particular, the normally observed ceramic wear mechanisms, adhesion (10), and abrasion (11), can be mitigated by environmental factors. Adsorbed water, for example, can promote near-surface plasticity leading to a soft surface layer some 1-10 micrometers thick. This soft surface layer seems to prevent adhesion and to lubricate ceramics as they slide over each other. For alumina sliding against alumina, it was observed that the coefficient of friction rose from 0.25 to 0.8 as the temperature of friction experiments was raised from room temperature to 400°C, driving off adsorbed water (12); introduction of moist air then produced an immediate reduction of μ_F. Adsorbed organic substances also tend to lubricate and soften the surface of ceramics. Myristic acid, for instance, enhances surface plasticity and suppresses cracking during sliding of steel on lithium fluoride (13). Chemisorbed oxygen appears to reduce the friction coefficient of titanium carbide by one-half (14).

Particularly pertinent to the present study is the work of Shimura and Tsuya (15), who investigated atmospheric and temperature effects on the friction and wear of several ceramics, including tungsten carbide, titanium carbide, chromium carbide, aluminum oxide, and their cermets. It was found that wear rates and coefficients of friction are higher in vacuum than in air. Based on characterization of the wear surfaces, the results were explained in terms of a postulated thin, soft lubricating surface layer which is formed by interaction of the ceramic/cermet with adsorbed moisture.

These results suggest that the intentional introduction of lubricious solid films, especially metal oxides, might provide ceramics with the ability to slide efficiently at elevated temperature. Delivery of such films, however, is a problem. Many ceramic coatings tend to fail via adhesion and delamination, so that any beneficial aspects of their presence are short-lived. However, Hirano and Miyake (16) have recently shown that adhesion during sliding contact may be reduced by ion implantation of both metal and inert ions. If such layers were, in addition, of a lubricious nature, they might be induced to provide transfer lubrication (17), i.e., continuous transfer of solid lubricant from one body to another during sliding contact. Ion implantation can, potentially, provide such layers, and by providing an intimate mix of implanted species and substrate, can produce a surface extremely resistant to adhesive delamination. Further, ion implantation provides a very thin "coating", so that well prepared surfaces maintain their original tolerance and finish.

B. Phase I Summary

Prior to exploring the possibilities of this idea, as outlined in the bulk of this report, simple ceramic-ceramic couples nominally compatible with the service requirements for seals (piston rings and cylinder liners) in a low heat rejection diesel engine were run in three pin-on-disk tests over a wide temperature range in both inert and simulated diesel exhaust environments. In such tests, the pins are considered to simulate moving piston rings, and the disks the stationary cylinder liner.

During this Phase I study, sliding friction coefficients and wear rates of promising carbide, oxide, and nitride materials were measured. Electron and optical microscopy were used to define the micromechanisms of wear, and X-ray spectroscopy was used to evaluate interface/environment interactions which seemed to be important in the friction and wear process. In order to determine the sensitivity of material properties to temperature and environment, the hardness and fracture toughness of candidate materials were evaluated from 23°C to 800°C in diesel exhaust and inert environments. Electric potential was varied in order to evaluate possible enhancement of friction and wear behavior via electrical effects. Results important in planning the Phase II experiments included the following.

Friction coefficients were quite high, ranging from 0.24 (NC 132/K162B in DE at 800°C) to 1.24 (NC 132/SiC in DE at 800°C). Plastic scoring seems to be significant in many of the wear mechanisms, suggesting that hardness is a controlling factor; however, friction coefficients are sensitive to environment, indicating the importance of factors other than plastic scoring (hardness) in the adhesion process. Wear of NC 132/TiC and NC 132/K162B is very low at all temperatures, due to the fact that TiC and K162B pins produce beneficial (low wear rate) films and oxides on both PSZ and K162B disks. Film/oxide formation clearly depended on disk/pin combination, temperature, and environment. Wear rates are low only when

either lubricating films or (possibly) rolling element particles (K162B/NC 132, 800°C, DE) are formed. Electric potential is not influential in modifying friction coefficients or wear rates.

C. Choices of Materials

The choice of ceramic materials for use in this investigation was based on the results of several studies (3,15,18-21) which strongly suggest that certain carbides are the outstanding candidates for high temperature piston rings. In particular, hot-pressed TiC, Ni-Mo bonded TiC cermets (3,18-21), and sintered SiC (20,21) have demonstrated favorable wear resistance and (relatively) low friction coefficients. Accordingly, these were selected as pin materials for the present experiments. Similarly, Si_3N_4, SiC, and partially stabilized zirconia (PSZ) are the most likely cylinder liner materials (21). Because of the extensive body of knowledge available regarding the former, and the attractive mechanical strength properties and minimal thermal conductivity of the latter, hot pressed Si_3N_4 and zirconia were selected as disk materials. Properties of the bulk ceramics selected for testing are given in Table I.

Metal species for ion implantation included chromium, cobalt, nickel and a double layer of nickel and titanium. These choices were based on: 1) the results of the unimplanted ceramic-ceramic tests, which led to the selection of TiNi and Ni; and 2) work reported in the literature (22) which seemed to indicate possible lubricious properties for oxides of cobalt and chromium. As will be shown subsequently, the best results for unimplanted sliding pairs corresponded to the transfer, from pins onto disks, of metal oxides to form discontinuous, but relatively lubricious, films. Unfortunately, this wore the pins significantly, and did not produce uniform lubrication. Therefore, it was decided to pre-implant candidate films into the disks, in the hope that they might transfer to the pins, while maintaining a minimal wear disk surface.

D. Ion Implantation

The implantation process used* was actually a variant known as ion mixing. In this technique, a thin coating of metal is vapor deposited onto the ceramic substrate, and argon ions are accelerated through a potential field, driving the deposited metal atoms into the substrate. In the case of the TiNi implant, Ni was first deposited, followed by the Ti; both layers were then simultaneously ion mixed.

The argon ions were accelerated using a beam voltage of 140 keV, with a fluence of 1×10^{17} ions/cm^2, and a flux of $\sim 10^{12}$ ions/cm^2-s. Implant layer thickness was estimated to be on the order of $\lesssim 400$ nm, based on subsequent Auger analysis.

*Westinghouse R&D Center, Pittsburgh, PA.

TABLE I

MATERIAL PROPERTIES

Material	E (GPa)	H (GPa)	K_{IC} ($MNm^{-3/2}$)	Grain Size (μm)	Tensile Strength (MPa)
SiC(1)	380	32	4.4	3-5	345
HP TiC(2)	450	32	5.0	30	~260
TiC-Ni-Mo (K162B)(3)	407	12	~15	3	1587
Si_3N_4 (NC 132)(4)	310	19	4.8	0.5-3	810
Partially stabilized zirconia (PSZ)(5)	210	10	8-15	60	600

(1) Carborundum sintered alpha SiC.

(2) Ceradyne, Inc.

(3) Kennametal Corporation.

(4) Norton Company.

(5) Nilsen (Nilcra) TS grade PSZ.

E. Friction and Wear Testing

A special wear testing machine was constructed to permit testing under conditions that are pertinent to the service environment of sliding seal materials in the adiabatic diesel engine. As sketched in Fig. 1, the basic configuration of the machine was that of a rotating disk against which three flat-ended pins of identical material slide under controlled normal force. The pin and disk assembly were housed within a heated environmental chamber. Since the pins suffered continuous sliding, while any point on the disk surface experienced only periodic passage of a pin, the pin materials operated under conditions similar to those imposed on a sliding seal ring, and the disk material experienced conditions analogous to those of cylinder liner materials.

Testing was performed from 23°C to 800°C, in both argon and simulated diesel exhaust environments, although most of the ion-implant tests were carried out at 800°C in the diesel exhaust environment. The latter consisted of 7.8% CO_2, 8.9% O_2, and the balance N_2; both diesel exhaust and argon environments were maintained at 276 kPa pressure. Disks and pins were run-in at temperature for five minutes at the start of each test, following initial evacuation and purging of the system with either diesel exhaust or argon and a minimum 20 minute pre-test soak at test temperature. Each test was performed under a static load of 22.5N, with the disk rotational speed at the point of pin/disk contact being 1 m/s. Run time ranged from 40 minutes to one hour.

F. Wear Characterization

Scanning electron microscopy was used to characterize wear mechanisms, while scanning Auger electron spectroscopy (AES), and energy dispersive spectroscopy (EDS) were employed to characterize wear particles and transfer layers. Surface profilometry was used as a measure of relative material loss. Because of problems associated with chipping and oxidation, wear rate determination by the measurement of specimen weight change was frequently compromised.

Prior to testing, both pins and disks were carefully polished to a 0.5 μm diamond finish. There was always, however, a slight mismatch in parallelism between pins and disk once a test began, and so on each pin, a small wear flat was produced (tests did not begin until this flat was run-in and basically stable). For subsequent wear characterization, the polished surfaces provided reference "no-damage" regions, while the boundaries of the pin flats constituted regions in which damage development could be observed from its inception to equilibrium wear. Similarly, the width of the annular wear track on each disk slowly expanded with the pin flats, so that again, by tracking across the boundary one passed quickly from no damage through the various stages of damage development leading to equilibrium wear.

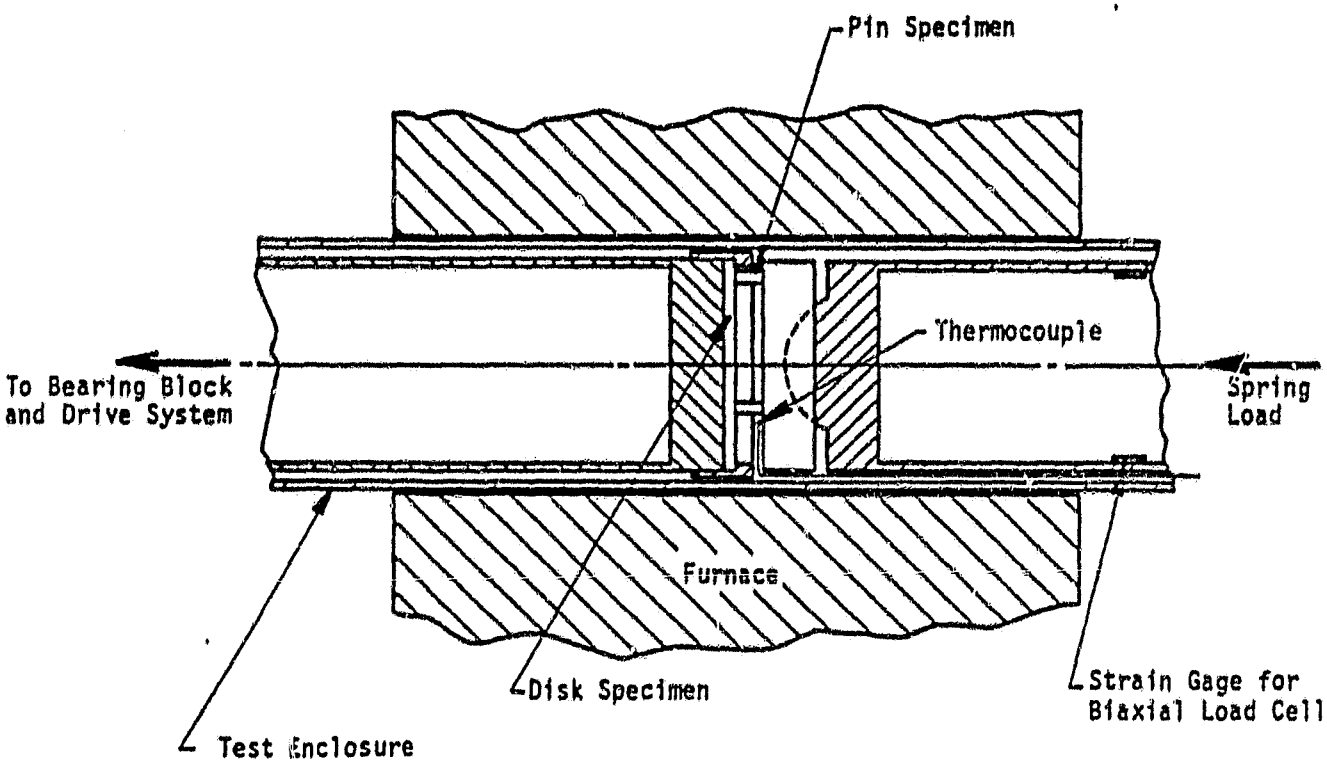

Figure 1. Schematic of Test Setup.

G. Results

1. Friction Coefficients

Friction coefficients μ for a typical ceramic-ceramic pin/disk couple in diesel exhaust and argon are shown as a function of temperature in Fig. 2; scatter bands indicated were characteristic of all couples tested. A more effective mode of presentation for subsequent discussion is to combine the curves for all three pin materials sliding on one disk in a given environment as in Figs. 3-6. For example, μ lies between 0.6 and 0.8 for all three pin materials run against zirconia in argon (Fig. 3). For Si_3N_4 disks in the same environment (Fig. 4), the situation is only marginally different; as the temperature increases, μ_F for all pins decreases slightly from ~ 0.8 to ~ 0.6. This simple behavior is altered drastically, however, by running in diesel exhaust environment.

As shown in Fig. 5, for zirconia disks in diesel exhaust μ rises rapidly with temperature for SiC and TiC, peaks at ~ 400°C, and then decreases rapidly with further increase in temperature. For TiC-Ni-Mo pins on the other hand, μ_F decreases monotonically from its initial room temperature value of ~ 0.9, to a low of ~ 0.45 at 800°C. For Si_3N_4 disks in diesel exhaust (Fig. 6), the TiC-Ni-Mo material behaves much as it does for zirconia disks in the same environment, dropping from ~ 0.75 at 23°C to 0.24 at 800°C. However, $\mu_F(T)$ for SiC and TiC increase monotonically; there is no mid-temperature peak, and at 800°C, μ_F is quite high for both.

Since most of the ion-implanted disks were run at a single, elevated temperature (400°C), it is most convenient to consider the corresponding friction coefficients as shown in Fig. 7. Clearly, ion-implantation with Cr is no more beneficial to friction behavior than is the use of unmodified ceramic couples. However, TiC-Ni-Mo pins run against zirconia disks implanted with TiNi and with Co have coefficients of friction of 0.09 and 0.06, respectively. Similarly, TiC pins with Si_3N_4 implanted with TiNi exhibit a coefficient of 0.09. These are extremely low friction coefficients, lying in the upper end of the range of values normally achieved through conventional liquid lubrication at low (<300°C) temperatures.

It is interesting to note that for TiC pins run against Ni-implanted silicon nitride, μ_F was ≥ 0.14, considerably worse than the value of 0.09 obtained for the TiNi-implanted case. Also, it is obvious that good friction coefficients are very sensitive to the precise nature of the couples. Titanium carbide was much worse than NiMo-bonded TiC against TiNi-implanted zirconia, while for TiNi-implanted Si_3N_4, the NiMo-TiC was superior (lower μ_F) to the TiC.

2. Wear Characterization

For non ion-implanted ceramic-ceramic couples, by far the most commonly observed wear mechanism was delamination parallel to the sliding direction. Radial cracking/chipping, in fact, was observed in only one

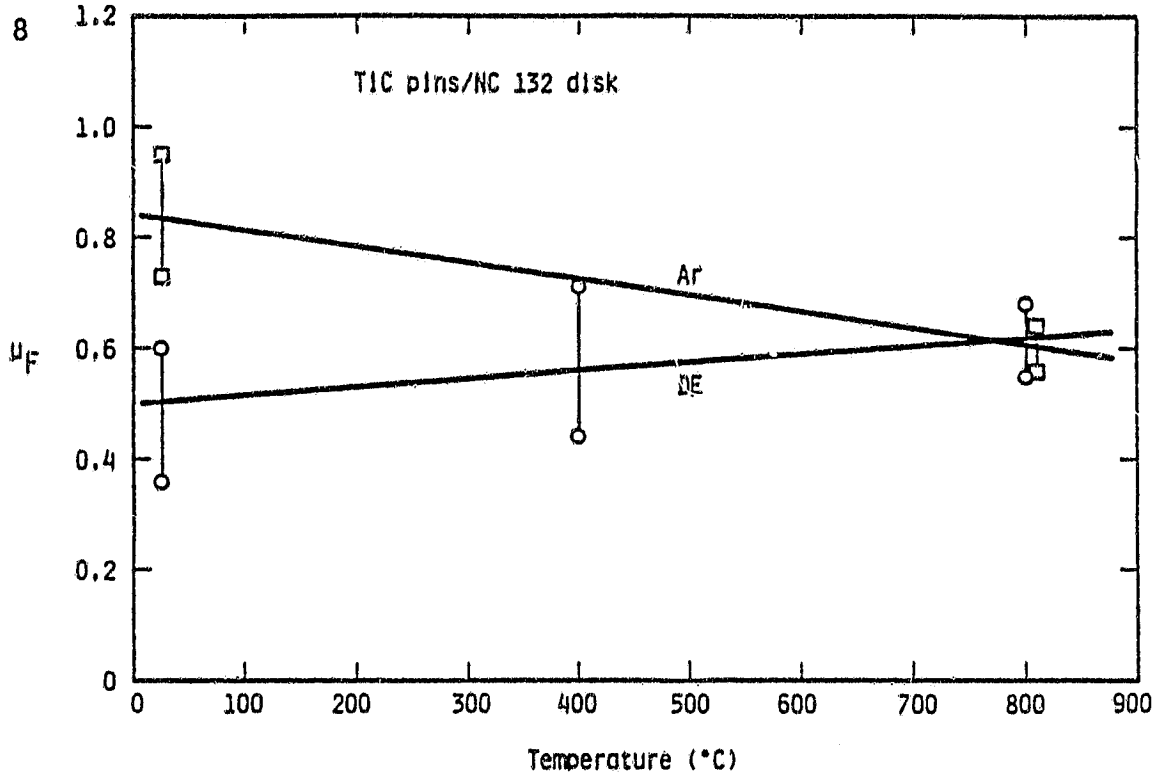

Figure 2. Friction Coefficient Versus Temperature for TiC Pins/NC 132 Disk in DE and Ar.

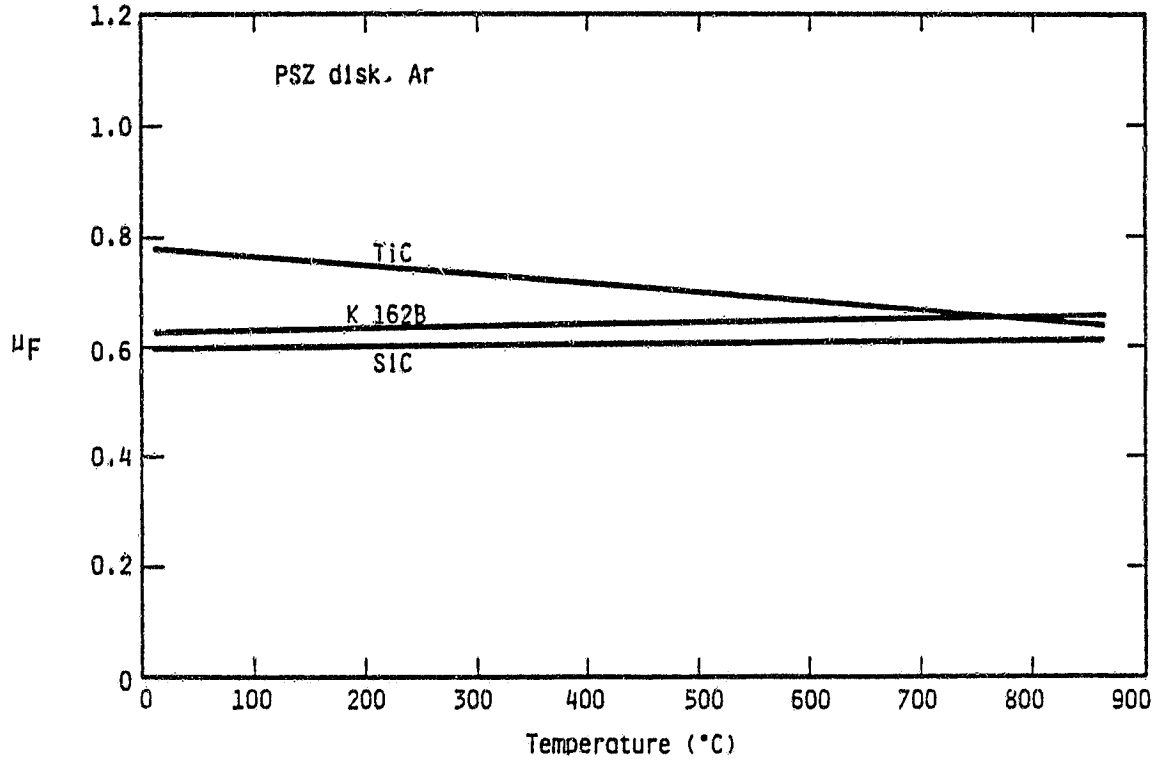

Figure 3. Friction Coefficient Versus Temperature for All Pin Materials on PSZ Disks in Ar.

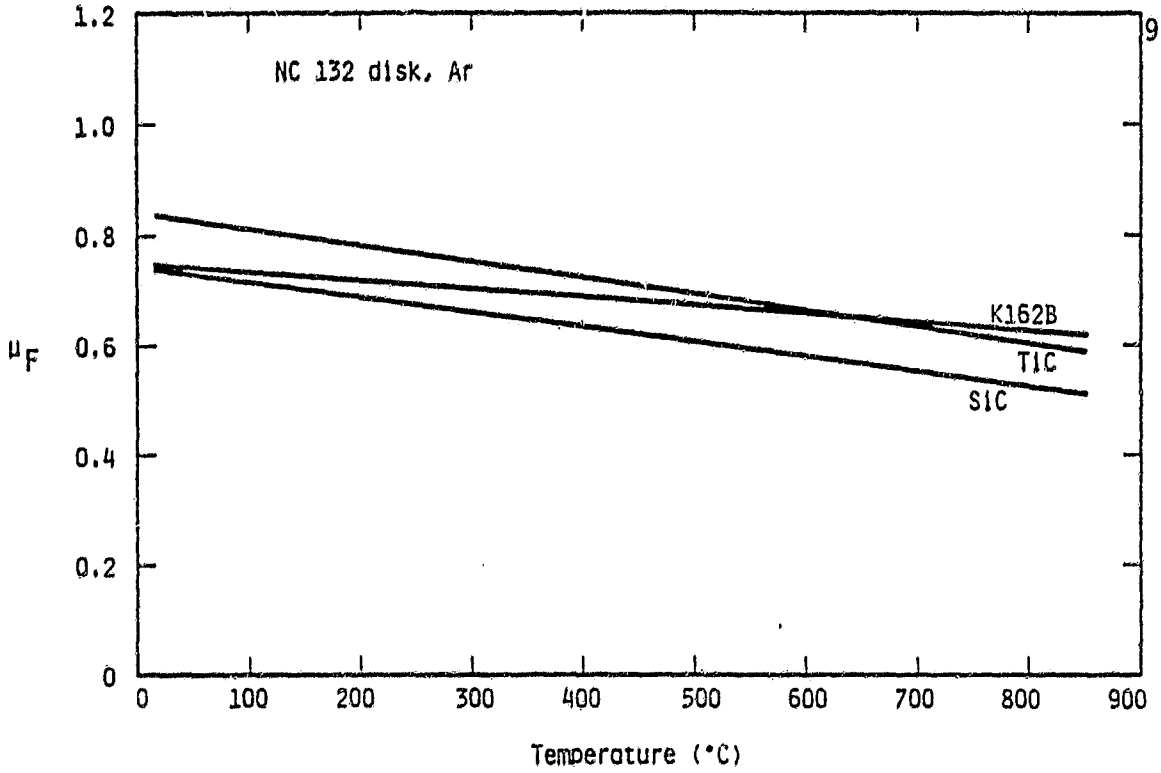

Figure 4. Friction Coefficient Versus Temperature for All Pin Materials on NC 132 Disks in Ar.

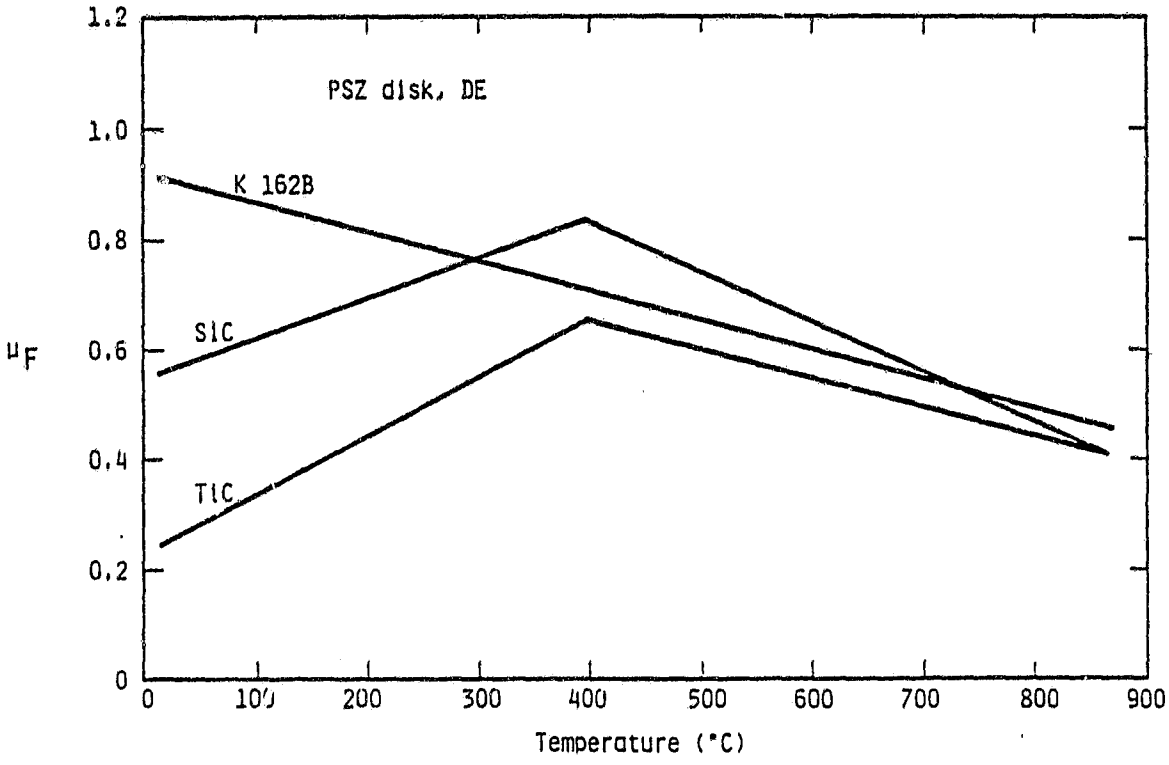

Figure 5. Friction Coefficient Versus Temperature for Pure PSZ.

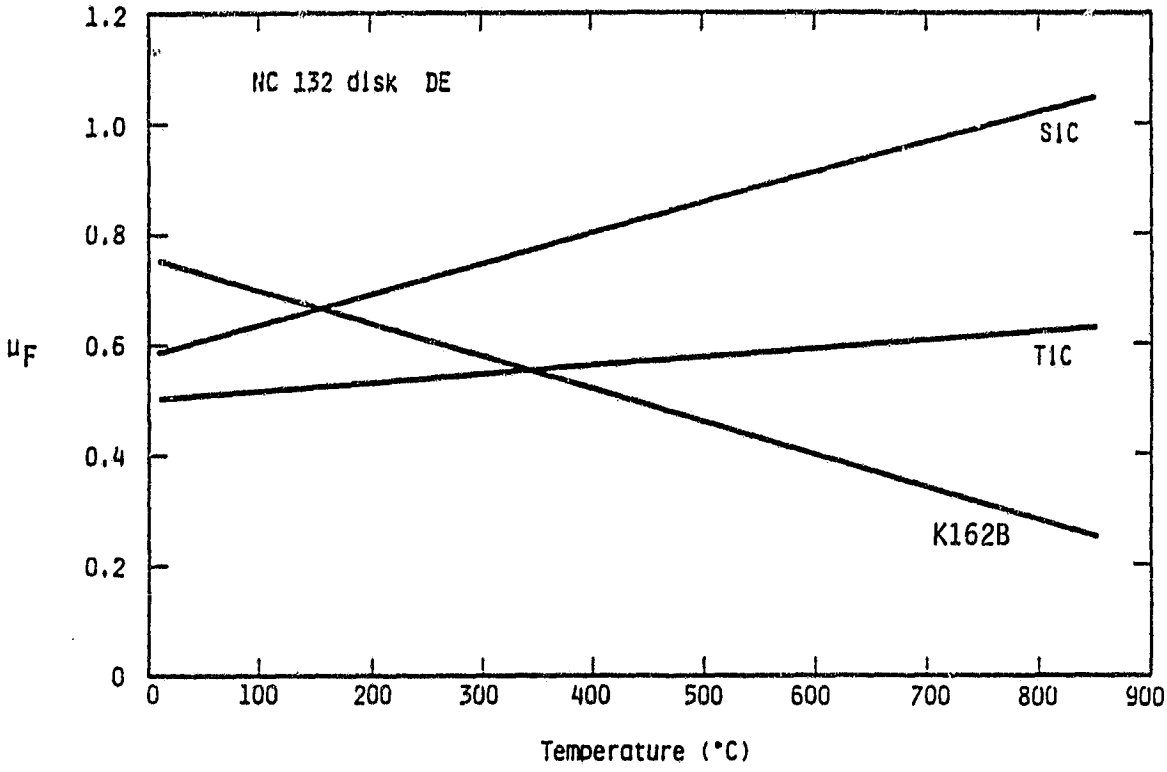

Figure 6. Friction Coefficient Versus Temperature for Pure NC 132.

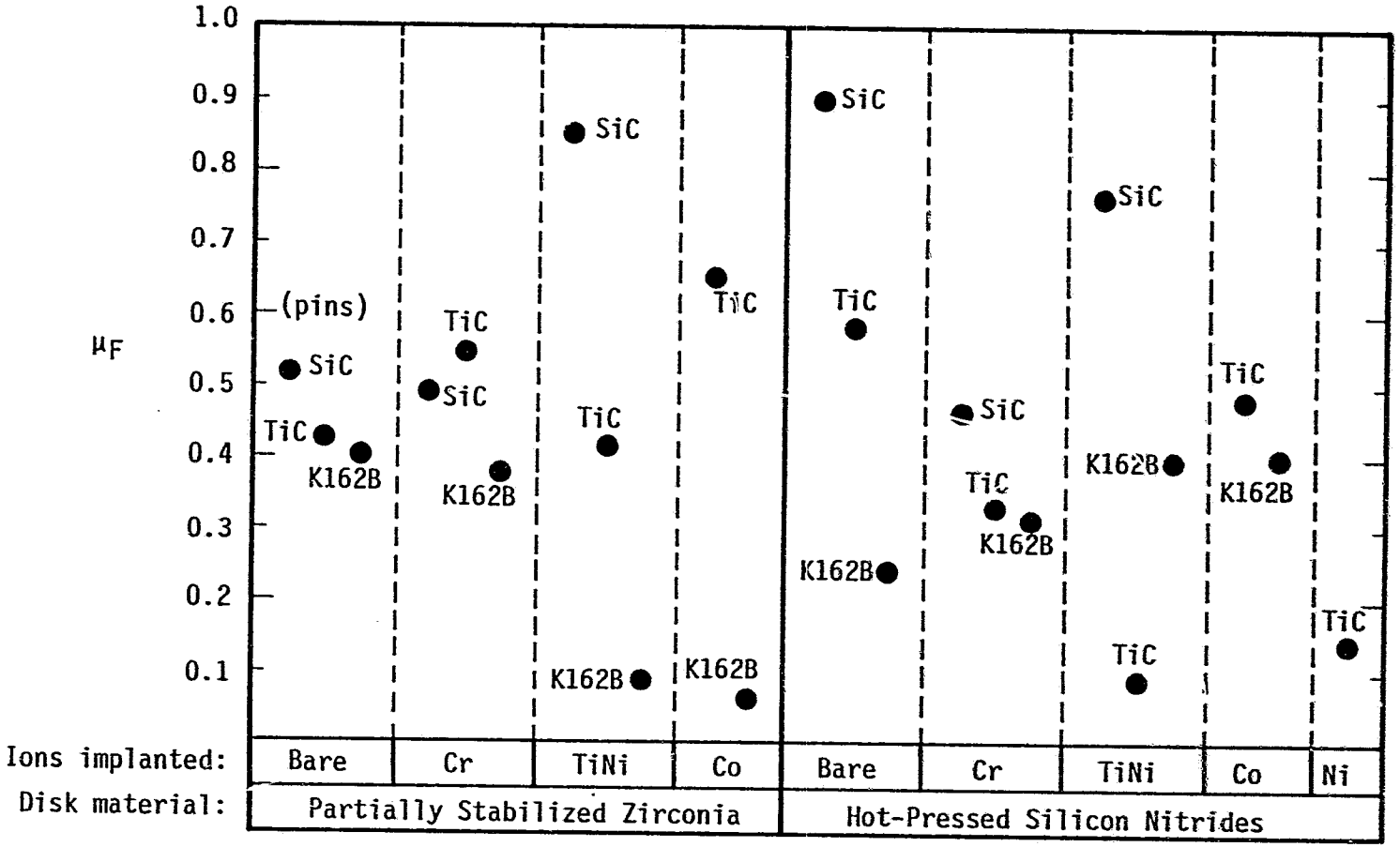

Figure 7. Steady-State Coefficient of Friction at 800°C in DE.

instance, i.e., for SiC pins sliding on an Si_3N_4 disk at 23°C in diesel exhaust environments. The cracks penetrated at a fairly steep angle, and interacted to form irregularly-shaped chips (Fig. 8). The Si_3N_4 disk on the other hand, manifested the much more commonly observed wear mechanism of delamination, the early stages of which are associated with the edges of plastic wear tracks.

As an example of this process, the development of delamination in Si_3N_4 and zirconia disks can be seen in Fig. 9, which shows several aspects of the process. In Fig. 9a, the delaminations have formed after no more than a few passes. Close study of equilibrium wear regions (Fig. 9b) shows that they are composed of thin sheets in the process of being removed (Fig. 9c). Delaminated sheets of zirconia can often be found lying at random on the disks and on the pins.

Delamination-type disk wear similar to this prevailed in all tests involving SiC pins, and for all tests involving zirconia in argon. In all of the other tests, which tended to correspond to lower friction coefficients, erosion occurred primarily by pin delamination combined with the transfer of pin material, either titanium oxide in the case of TiC pins, or titanium and/or nickel oxide*, in the case of NiMo-bonded TiC (molybdenum never was transferred, since at 800°C Mo rapidly volatilizes as MoO_3). An example of such a film transfer process is shown in Fig. 10, in which TiO_2 has transferred from TiC pins to Si_3N_4 disks at 23°C and 800°C in the diesel exhaust environment.

Before discussing the wear behavior of the ion-implanted material, it is instructive to consider the nature of the implanted "coatings". As shown in Fig. 11a, the Ti and Ni are mixed together reasonably well, but contain relatively little of the underlying Si_3N_4 (indicated by the Si profile). Some oxygen is present near the surface, predominantly within the Ti-rich portion of the "alloy". However, after a 30 minute soak at 800°C in the diesel environment (Fig. 11b), both the Ti and, especially, the Ni, have diffused together, oxidized, and mixed with the Si_3N_4. The thickness of the implanted coating is estimated, on the basis of previous sputtering rate work, to be around 0.40 μm. Further discussion of this point is given in Section II.

During wear tests, the pins oxidize, and then develop small wear zones where they have been in contact with the ion-implanted disks. An example of such a zone is shown in Fig. 12 for a TiC-Ni-Mo pin run against TiNi-zirconia. Based on the sizes of such zones, the contact stress was typically on the order of 3.5-7 MPa.

Inspection of the "wear zones" shows that they actually do not represent pin wear; instead, they are thin lubricating films transferred

---

*We shall use TiO_2 and NiO to indicate these oxides, although the exact stoichiometry was not determined.

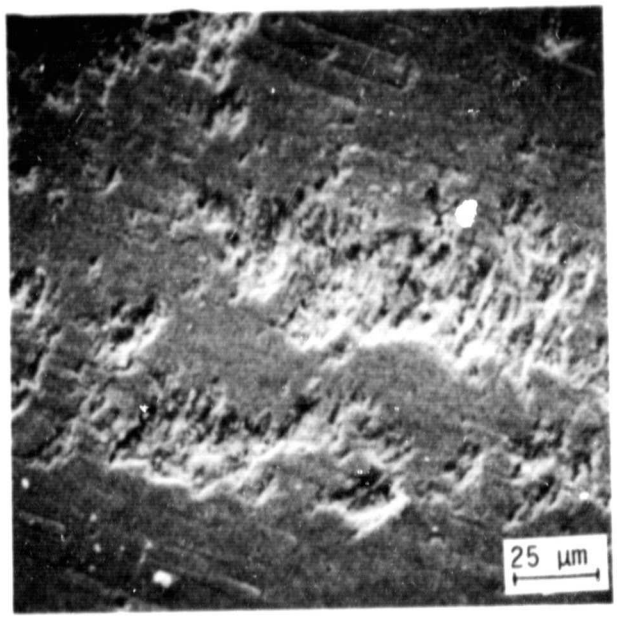

(a) Initial wear.

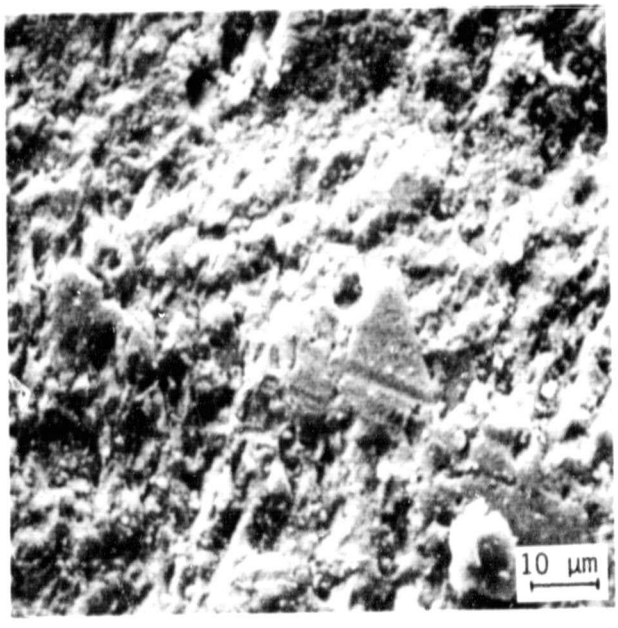

(b) Equilibrium wear.

Figure 8. Radial Crack Wear Particle Formation in SiC Pin Run Against NC 132 at 23°C in DE.

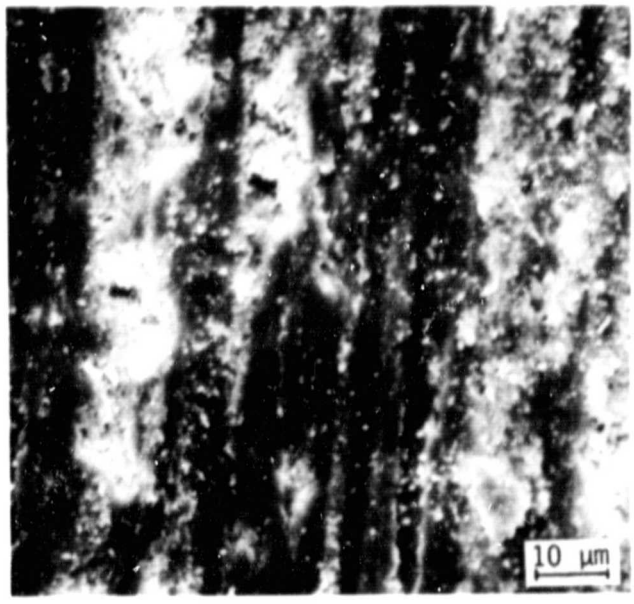

(a) NC 132 disk (SiC pins)

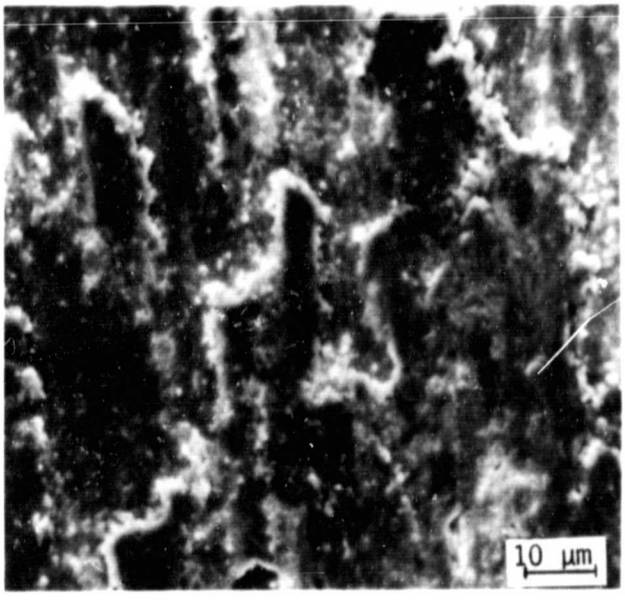

(b) PSZ disk (SiC pins)

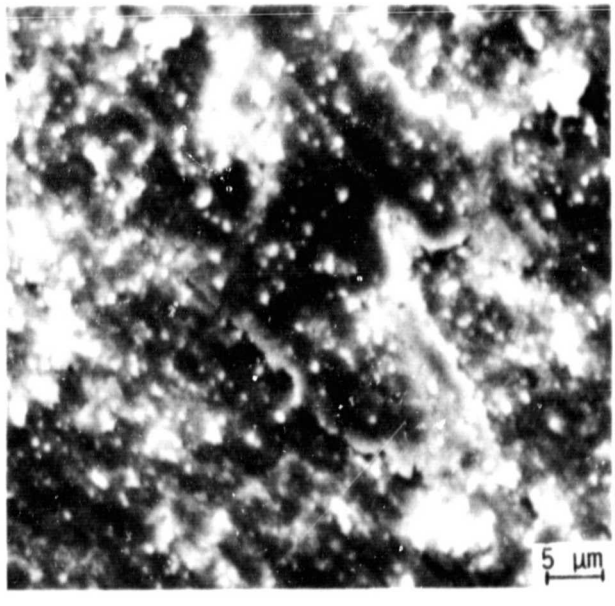

(c) PSZ disk (TiC pins)

Figure 9. Examples of Delamination in NC 132 and PSZ Disks, 23°C in DE.

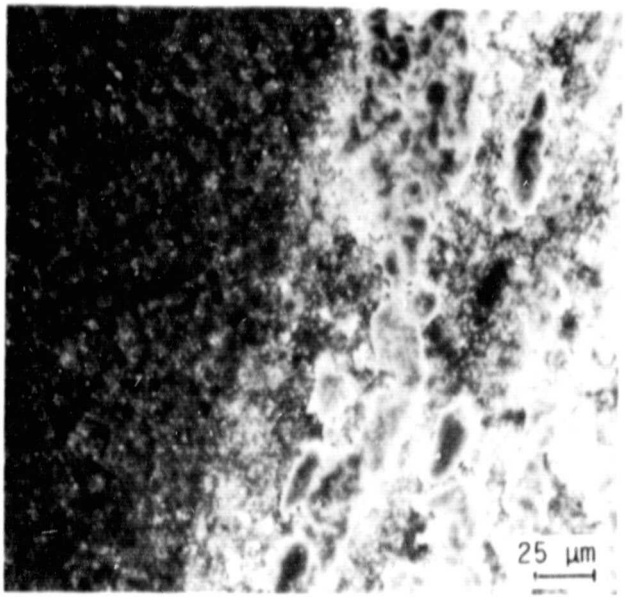

(a) TiO_2 deposit, disk, 23°C

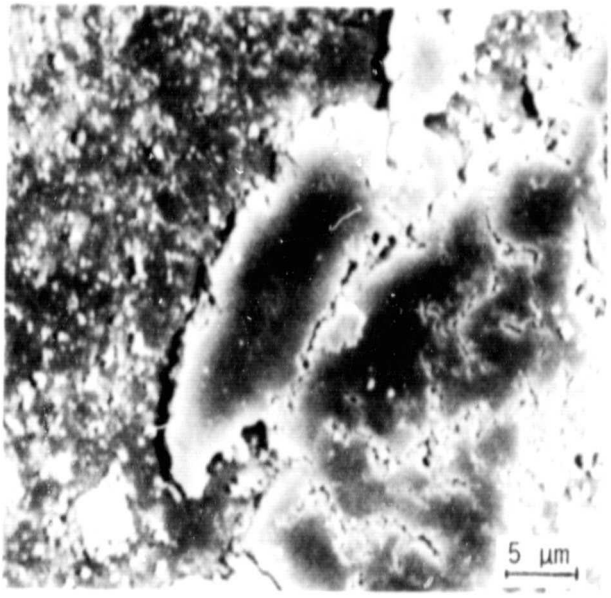

(b) Details TiO_2 deposit, disk, 23°C

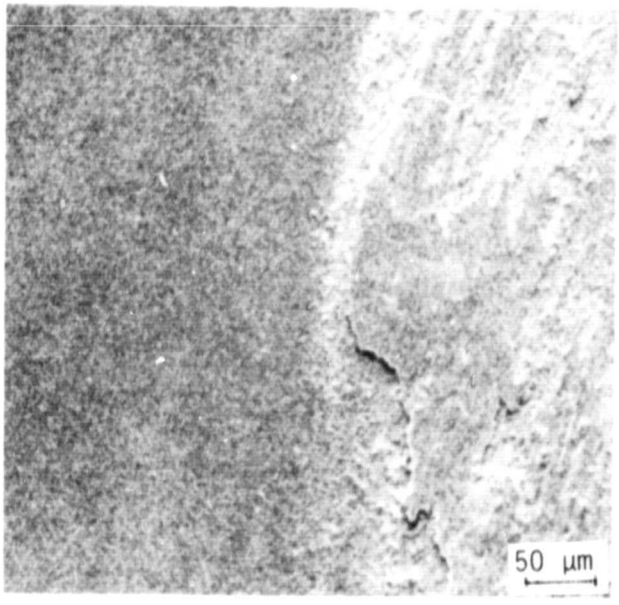

(c) TiO_2 deposit, disk, 800°C

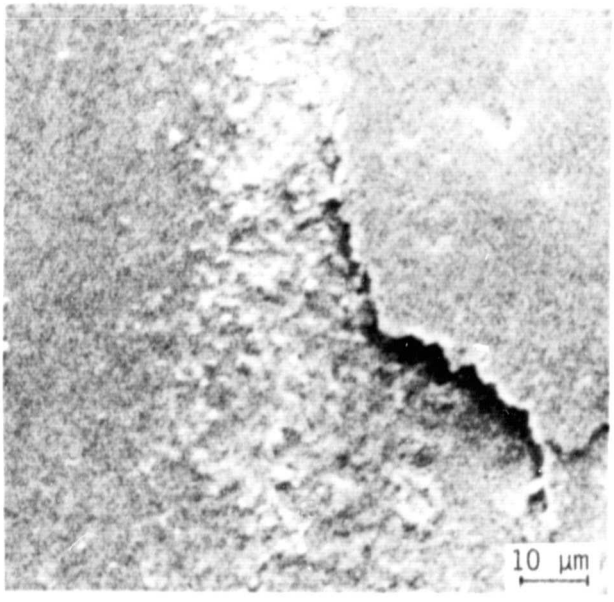

(d) Details TiO_2 deposit, disk, 800°C

Figure 10. TiO_2 Deposits on NC 132 Disks Run Against TiC Pins in DE.

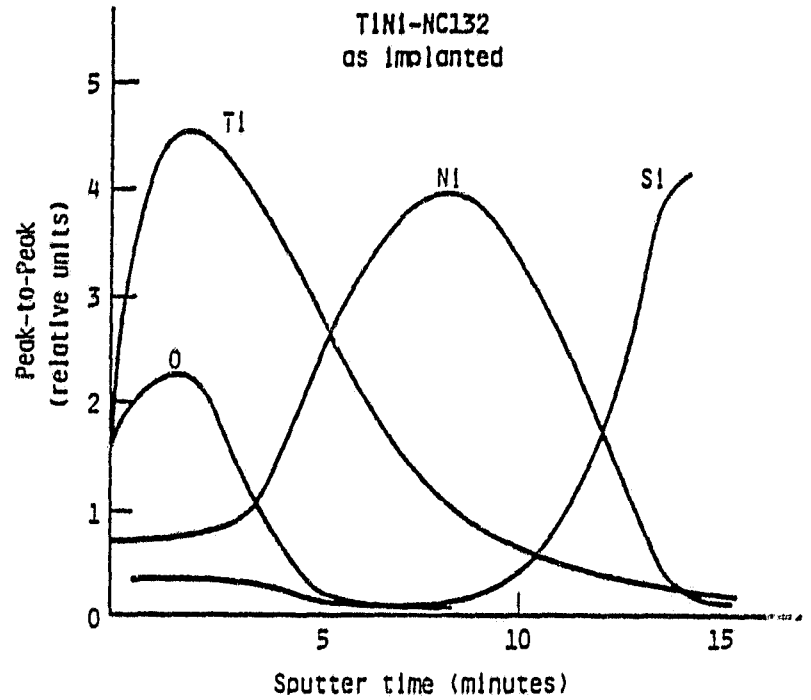

(a) As-implanted elemental distribution.

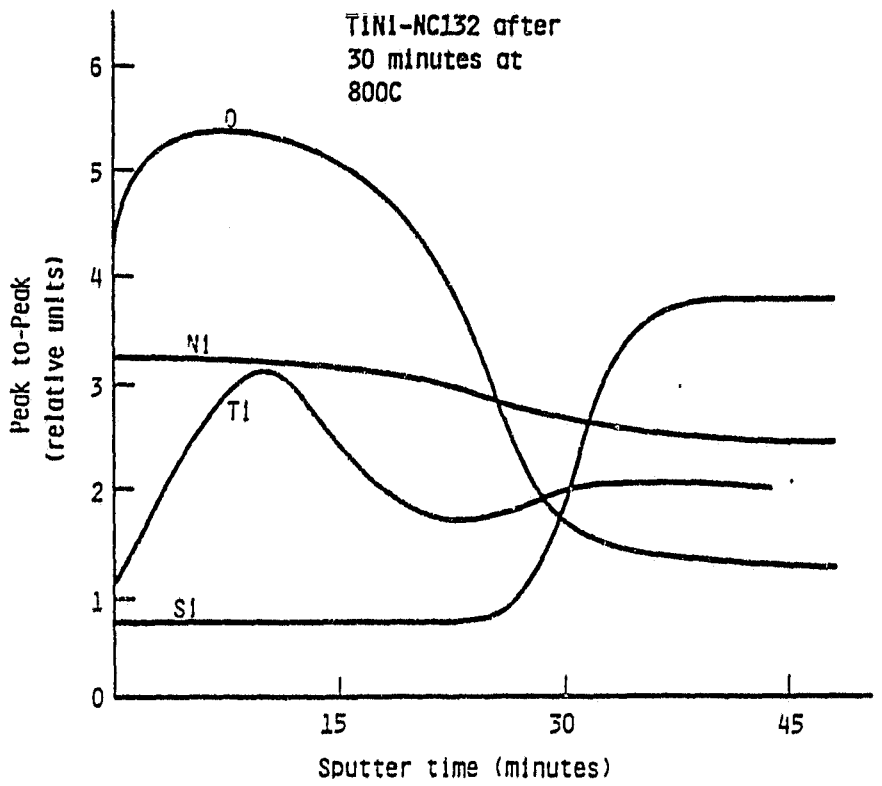

(b) Elemental distribution after 30 minutes at 800°C in DE.

Figure 11. Scanning Auger Analysis of TiNi Ion-Implantation in NC 132.

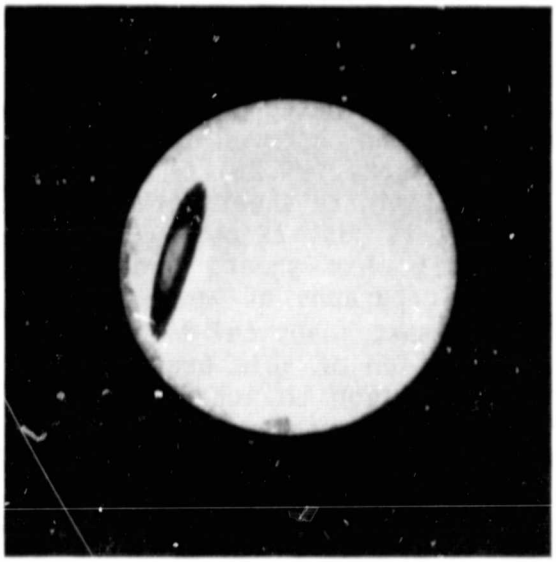

Figure 12. Wear Zone (Deposits) on K162B Pin Run Against TiNi-PSZ.

from the ion-implanted disks. Auger spectroscopy, which is discussed in detail in Section II, indicates that the films are composed of TiO_2 and NiO. Similar results were found for the Co-implanted zirconia disks tested against TiC-Ni-Mo pins, i.e., CoO was transferred from disk to pin.

H. Discussion

When disk (and heavy pin) wear was observed, it usually was in the form of delamination. This is a form of adhesive wear, in which intermittent contact nucleates shallow subsurface cracks which eventually grow to the surface, creating a thin delaminated sheet of material. This is similar to delamination which has been observed in metals (23) and in ceramics (1), and modeled based on a theory (24,25) of cyclic crack growth. However, in the present case, delaminate sheets often form within only a few, possibly even one pass. This is just as observed by Yamamoto and Buckley (26) for 304 stainless steel wear sheets produced by sliding against Al_2O_3. In fact, the photomicrographs of wear layers in the steel alloy studied by the latter look almost identical to those observed (Fig. 9) in the present ceramics. Prevention of this process must involve either 1) provision of sufficient lubrication to inhibit ceramic-ceramic adhesion, and/or 2) increase in the near-surface crack growth resistance of the delaminating material.

Although the friction coefficients of all of the unmodified couples exceeded 0.2, there were encouraging results regarding wear resistance. For those cases in which TiC or TiC-Ni-Mo material was transferred to disks in the form of titanium oxide films, disk wear was essentially nonexistent (unmeasurable via surface profilometry), and pin wear did not appear to be high once the initial sacrificial material transfer was accomplished. Apparently these films, which can form from room temperature to 800°C, are lubricious, in terms of wear.

The true potential of the films, of course, seems to have been realized by first ion-implanting and then oxidizing the disks. Under these circumstances, titanium oxide, nickel oxide, and cobalt oxide transfer selectively, i.e., from certain disks to certain pins (Figs. 13 and 14), and serve as liquid-like lubricants at the operational temperature. Based on the results of Breznak, et al (1), it would be reasonable to suspect that the temperature rise at the sliding interface was at least 300°C, hence the lubricant temperature probably was at least 1100°C. This should be sufficient to significantly enhance the viscosity of a ternary or quaternary alloy (oxide). In this regard, it is interesting to note that the friction coefficient of Ni-implanted Si_3N_4 run against TiC in diesel exhaust was 0.14 at 800°C, but rose to 0.4 when testing was performed at room temperature. Evidently the NiO, which was observed to transfer during sliding, was not sufficiently hot at 23°C (plus ~ 300°C due to sliding contact) to serve as an effective lubricant.

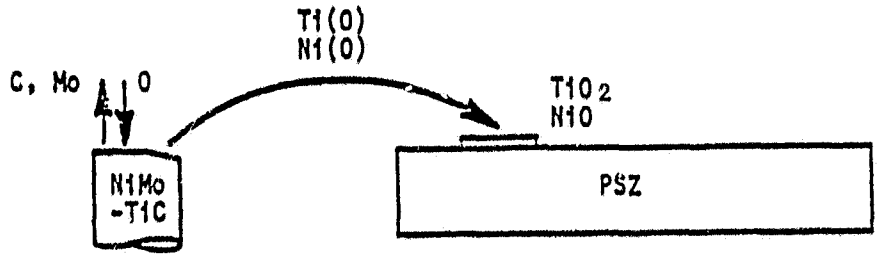

(a) Pure PSZ

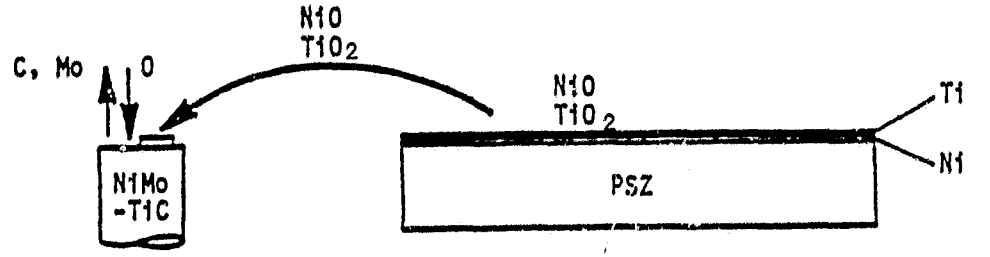

(b) TiNi-Implanted PSZ

Figure 13. Film-Lubricant Transfer in the NiMo-TiC/PSZ Systems.

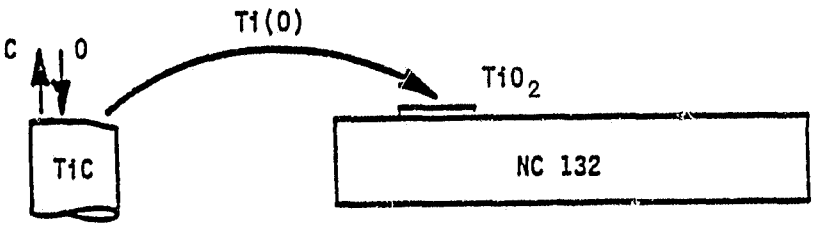

(a) Pure NC 132

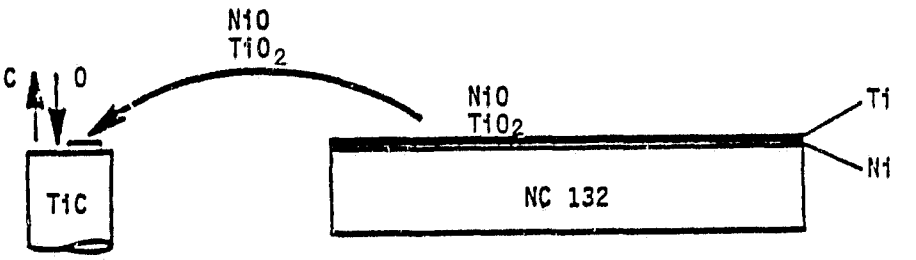

(b) TiNi-Implanted NC 132

Figure 14. Film-Lubricant Transfer in the TiC/NC 132 Systems.

It should be borne in mind that work to date has emphasized relatively short term tests designed to screen, and provide specimens to evaluate, the best pin-disk couples. It will be very important to evaluate the ability of the self-lubricating couples which have been identified to maintain their desirable traits over extended operating time.

I. Conclusions

Friction and wear tests have been conducted on a variety of ceramic/ceramic couples in the unmodified state or surface modified by ion implantation in both argon and an environment typical of high temperature adiabatic diesel engines. It has been found that:

- Low friction coefficients of unmodified ceramic couples correspond to the formation of lubricious oxide films.
- Oxide film formation depends on disk/pin combination, temperature, and environment.
- The most common and destructive mode of wear is delamination.
- For unmodified ceramic pin/disk combinations, the lowest friction coefficient obtained was 0.24.
- Ion implantation of disks with TiNi or Co reduces coefficients of friction at 800°C in simulated diesel exhaust environment to 0.06-0.09, for certain specific pin-disk combinations.
- The latter combinations appear to be attractive piston ring/liner candidates for the adiabatic diesel engine.

II. CHARACTERIZATION OF ION-IMPLANTED CERAMIC WEAR SURFACES USING AUGER ELECTRON SPECTROSCOPY

It is clear that the conditions present at the contact interface between the pins and the disks, and the chemical and mechanical processes occurring there determine the overall friction and wear behavior of the various ceramic pin-disk combinations. In order to determine the role of interfacial properties on the friction and wear behavior of the more promising ion-implanted ceramics, surface analysis techniques were used to examine the properties of the wear surfaces on the pins and on the disks. Scanning Auger electron microscopy was used to determine the chemical makeup of the wear surfaces, while scanning electron microscopy was used to investigate the physical properties of the wear surfaces.

A. Experimental Procedure

The pins and disks analyzed in this portion of the study are listed in Table II. Pin-disk combinations 1 and 4 with the titanium-nickel implant showed the best friction characteristics of those investigated during the friction and wear testing. Pin-disk combinations 2 and 3 showed less favorable frictional characteristics and a possible role of pin material in the wear process. The cobalt implanted and nickel implanted disks also showed promising results, although not as favorable as those of titanium-nickel implanted disks. These pin-disk combinations were therefore chosen for extensive analysis using Auger electron spectroscopy (AES). The results of AES or energy dispersive spectroscopy (EDS) analyses of the surfaces of other pin-disk combinations showing poorer wear characteristics will be discussed as necessary.

The investigations of the wear surfaces of both pins and disks listed in Table II were performed with a PHI 595 scanning Auger electron microscope. While Auger electron spectroscopy is now used routinely to investigate surface properties of metals, there are still unresolved problems when it comes to dealing with bulk semiconducting, or in this case, nonconducting materials. These include charging of the materials due to the accumulation of positive or negative charge at the analyzed region (27-28), and alteration of the analyzed surface by the electron beam, or by the ion beam during sputtering (28-29).

The problem of charging can manifest itself in two ways in scanning Auger microscopy: electrostatic charging which disturbs the secondary electron image as commonly found in secondary electron microscopy (30), and charge induced shifts in Auger peak positions (27-28,31). The charging of insulating samples is due to their inability to remove excess charge by conduction. In the case of electron microscopy, excess charge is created through the production of secondary electrons by the incident beam. The dependence of the secondary electron yield, δ, on the primary electron energy is shown schematically in Fig. 15. The energy range of interest for AES is that between the two crossover points, E_1 and E_2, where $\delta > 1$ (28,31). In this range, however, a net positive charge will

TABLE II

PIN-DISK COMBINATIONS TESTED IN DIESEL (O, N, CO_2, H_2O) ENVIRONMENT AT 800°C CHOSEN FOR SURFACE ANALYSIS*

	Disk‡	Pin‡	μ_F
1.	Silicon nitride Si_3N_4 (Ti,Ni)	TiC	0.09
2.	Silicon nitride Si_3N_4 (Ti,Ni)	TiC-5Ni-5Mo	0.22
3.	Partially stabilized zirconia PSZ (Ti,Ni)	TiC	0.25
4.	Partially stabilized zirconia PSZ (Ti,Ni)	TiC-5Ni-5Mo	0.09
5.	Partially stabilized zirconia PSZ (Co)	TiC-5Ni-5Mo	0.06
6.	Partially stabilized zirconia PSZ (Co)	TiC	0.25
7.	Silicon nitride Si_3N_4 (Ni)	TiC	0.14
8.	Silicon nitride Si_3N_4 (Ni) (tested at room temperature)	TiC	0.28

* The elements given in parenthesis are those ion-implanted into the surfaces of the disks.

‡ Specimen dimensions:

Disk diam. = 7.62 cm thickness = 0.95 cm
Pin diam. = 0.64 cm length = 1.27 cm

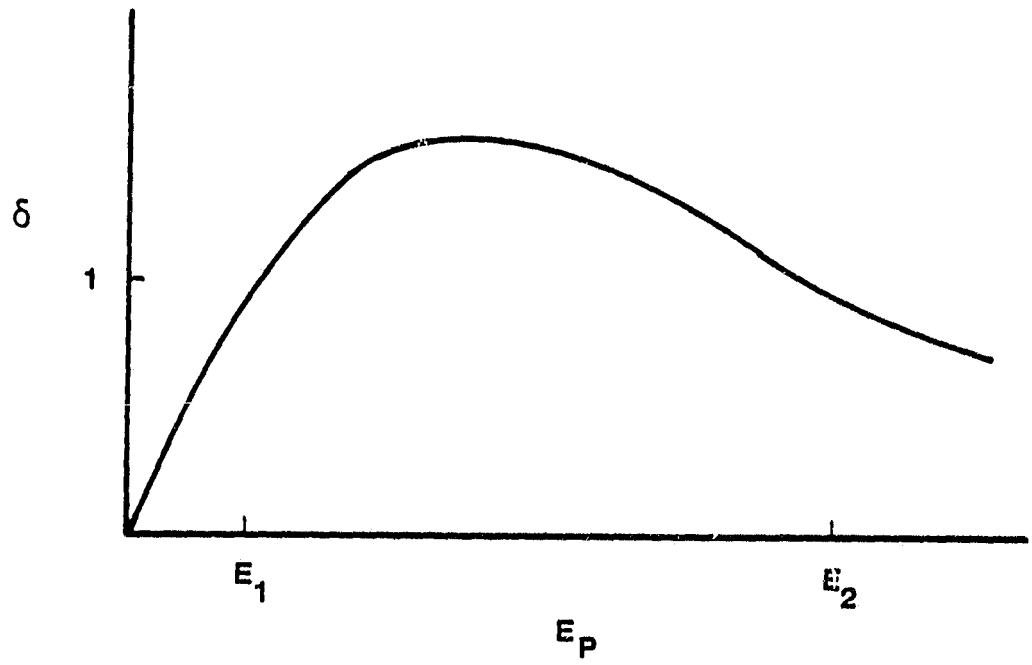

Figure 15. Schematic Diagram of Secondary Electron Yield as a Function of Primary Beam Energy.

build up at the surface of an insulating specimen because more electrons leave the specimen than are incident on it. This positive charge will retard the emitted Auger electrons and therefore cause a shift of the Auger peak heights to lower energies (31). This will cause little problem with normal elemental identification since surface charging should affect all Auger peak positions by the same amount. Some caution should be exercised, however, in analyzing Auger spectra for chemical information related to peak energy shifts. By considering the changes in the differences between Auger peak positions, rather than the absolute value of the peak positions, as well as the peak shapes, chemical binding information can still be obtained. However, alteration of surface chemistry by ionic drift as well as by electron beam heating must still be accounted for (28-29).

Several methods can be used to reduce the problem of charging of insulating specimens, although these require some sacrifice in resolution and sensitivity. The energy range E_1 to E_2 generally falls below 2kV for such materials, and therefore indicates that primary beam energies lower than those normally used for conducting specimens should be used (31). Reducing the irradiation dosage (C/cm^2) by reducing either the primary beam current or the analysis time can delay the onset of the maximum charging effect, as well as the onset of electron beam-induced damage (32). Reducing the angle of incidence results in a reduction of the secondary emission yield at a given beam condition, thus reducing charging (28,32). Non-beam related methods include coating the specimen in a conductor such as gold or silver while masking off a small area for analysis (30,33), or bombarding the specimen with a neutralizing beam (31). The neutralizing beam concept is also used for the reduction of charging during ion sputtering (31).

Alteration of specimen surfaces, either conducting or nonconducting, by the electron beam or ion beam sputtering can occur by electron beam reduction of the surface (32), migration of ionic species by charge buildup (29), beam heating (29,32), and preferential sputtering (34). These problems will have an important effect on the interpretation of quantitative and chemical Auger data. The results of this preliminary study are not greatly influenced by the surface alteration problems, but further work on the fundamental mechanisms of these wear processes will require careful consideration of these issues.

The major consideration for this study was the problem of surface charging. Use of primary beam energies above 2 kV, and beam currents above about 10^{-8} A resulted in secondary image distortion, and distortion of the low energy end of the Auger spectra, as well as random spiking throughout the spectra. It was found that a combination of the previously mentioned remedies could reduce the charging problem to a maximum shift of ~ -5 eV in the Auger spectra.

In the case of the disks, a thin film of silver was first vapor deposited onto the specimens. It was found that sputtering away an analysis area with concurrent elemental analysis was better than masking, since

even a small uncoated area seemed to charge up quickly. The specimens were then tightly wrapped in aluminum foil with a small area left uncovered for analysis, strapped to a specimen holder with copper wire, and mounted in the chamber. The disks were analyzed at the 60° angle of incidence set by the specimen holder in the 595 system at a primary beam energy of 1.5 kV, a beam current of $\leq 5 \times 10^{-9}$ A, and a beam size of < 450 nm. To avoid further charging, the beam was blanked while preliminary data handling and analysis was being performed. Depth profiling was performed using argon ion sputtering with a beam energy of 2 kV, current density of ~ 70 $\mu A/cm^2$, and a 2 mm x 2 mm raster size. The sputtering rate for the combination of materials used in this study was not known, and the depth scale is therefore given as sputtering time. Use of these sputtering conditions on a Ta_2O_5 film, however, gave a sputter rate of about 11.0 nm/min.

Because of the small size of the worn area of the pins and the fine scale of the features found there, the pins were not silver coated. They were, however, wrapped in aluminum foil, leaving the worn end uncovered. Examination at glancing incidence of the electron beam was required to avoid charging problems.

B. Results of Analysis on Titanium-Nickel Implanted Disks

1. Pins

All of the pins run against the titanium-nickel implanted disks exhibited an apparent burnish mark where the pin was in contact with the disk. The burnish marks of the pins with higher values of coefficient of friction, μ_F, were larger than those with lower values. A typical burnish mark from a TiC pin run against a Si_3N_4 (Ti,Ni) disk (low μ_F couple) is shown in Fig. 16a. It appears that the burnish mark is actually a layer of material which was transferred from the disk to the pin, and was then broken up later in the wear run. This is more clearly seen at higher magnification in Figs. 16b-c. Arrows indicate areas (usually darker) where the pin "base" material appears beneath the burnish layer. This mark will thus be referred to from this point on as a "transfer layer".

Typical Auger spectra from the unworn surface of the pin and the transfer layer are shown in Figs. 17a-d. The main difference between the two areas, as seen by comparing Figs. 17ab with 17cd, is the presence of nickel on the transfer layer. Since these spectra come from the TiC pin, the nickel could only have transferred from the TiNi-implanted disk to the pin. It is not clear whether or not the nickel is present in the oxidized state, because the peak energy and shape changes associated with the oxidation of nickel are too small to be resolved under the present specimen and beam conditions (39). Titanium, however, clearly is present in the oxidized state, as evidenced by the absence of the elemental Ti(27 eV) peak and the presence of the oxidized Ti(40 eV) peak (35), and the fact that the Ti(387 eV) peak is larger than the Ti(418 eV) peak (35-38).

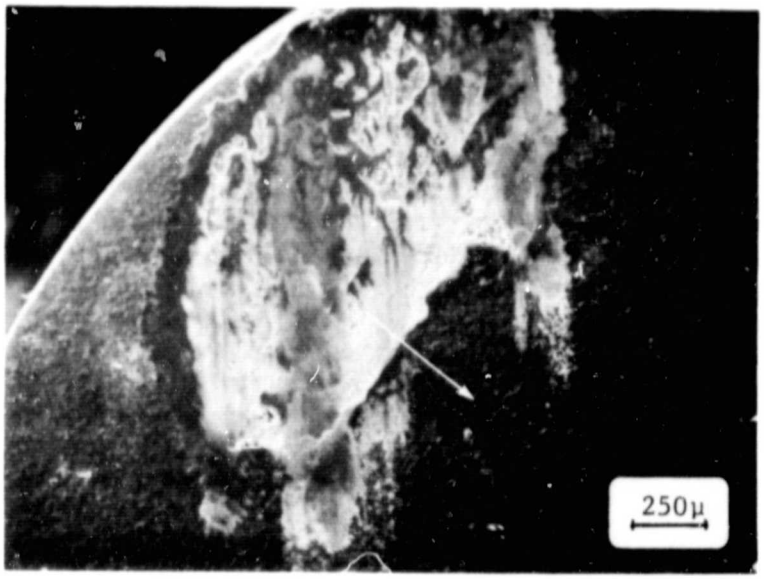

(a)

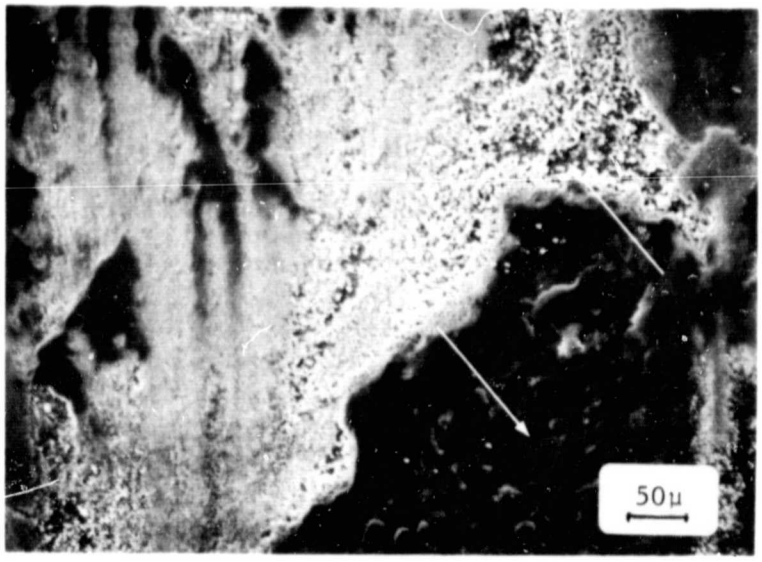

(b)

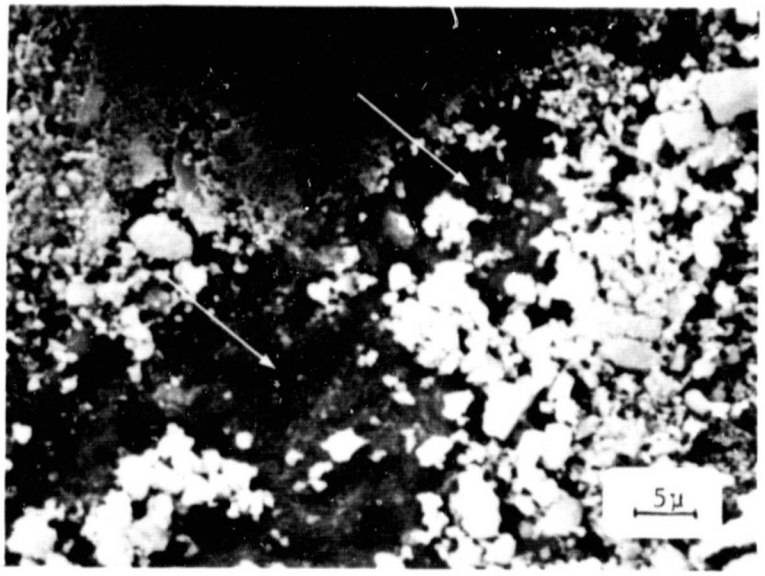

(c)

Figure 16. Transfer Layer on a TiC Pin Run Against a Ti, Ni-Implanted Disk in a Diesel Environment at 800°C. Arrows indicate pin "base" material.

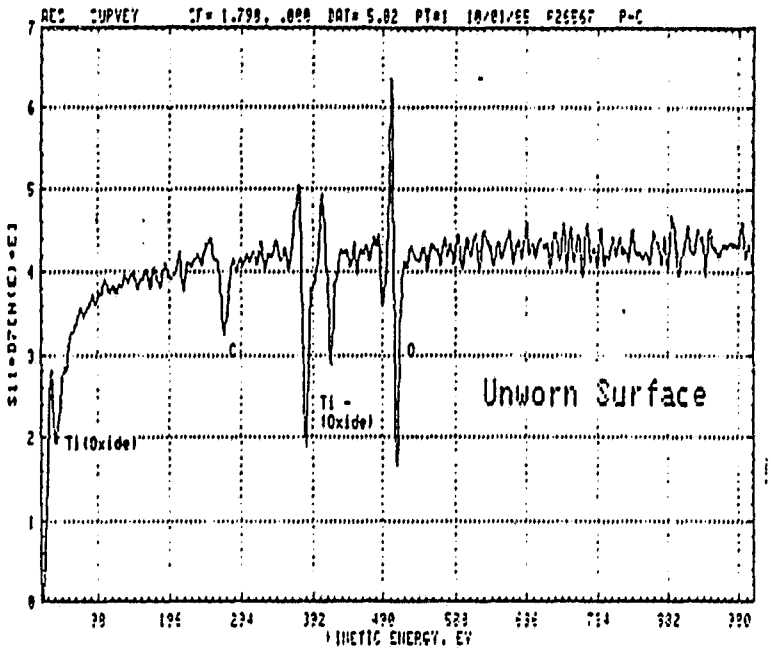

(a) Unworn surface.

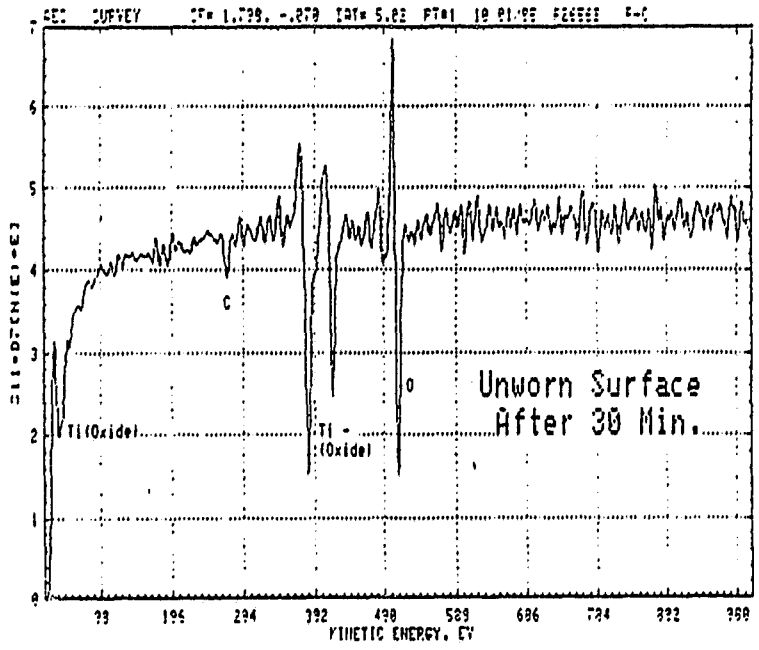

(b) Unworn surface after 30 minute sputter.

Figure 17. Auger Spectra Taken from a TiC Pin Run Against a Ti, Ni-Implanted Si_3N_4 Disk in a Diesel Environment at 800°C.

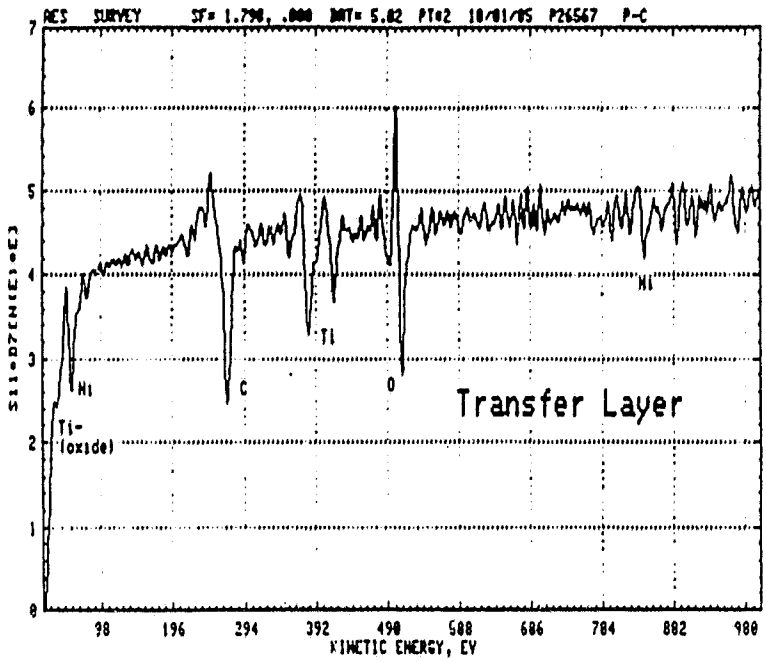

(c) Transfer layer.

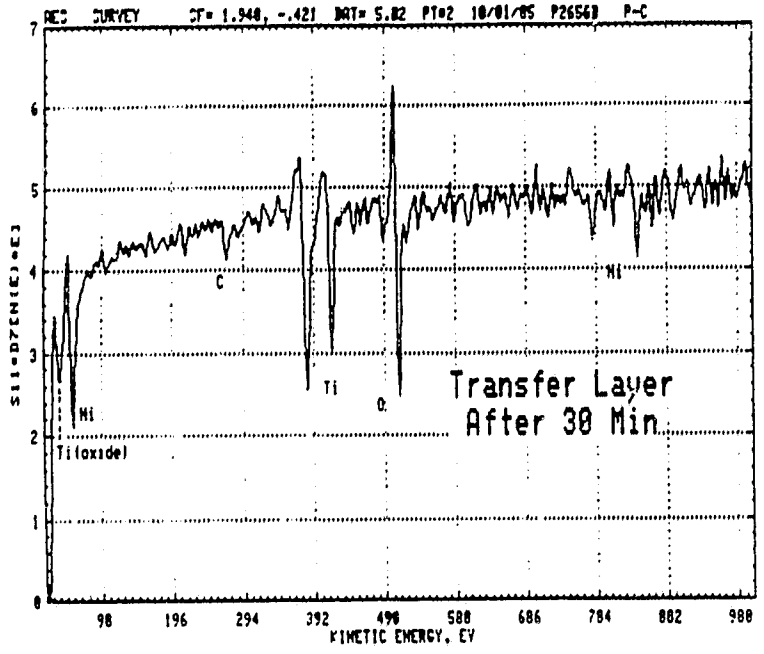

(d) Transfer layer after 30 minute sputter.

Figure 17 (Continued). Auger Spectra Taken from a TiC Pin Run Against a Ti, Ni-Implanted Si_3N_4 Disk in a Diesel Environment at 800°C.

Carbon is also present in significant amounts, with a greater amount of carbon being found on the transfer layer (Fig. 17a) than on the unworn surface (Fig. 17c); this is indicated by the larger peak height ratio C(272 eV)/O(510 eV) for the transfer layer. Sputtering of the pin surface resulted in a reduction of the carbon signal with depth, while the titanium oxide peaks remain strong. However, the presence of a small amount of carbon even after 30 minutes of sputtering indicates that this carbon layer consists of more than just carbon adsorbed during specimen handling. While the TiC pin is probably oxidized to a significant depth, this relatively thick carbon layer is probably the result of the interaction of the diesel environment with the pin surface, although some transfer of carbon originally implanted in the disks is also a possibility (see next section). The apparently higher surface concentration of carbon on the transfer layer would be due to the higher temperatures existing at the contact point, and/or the direct contact with the carbon-containing implanted layer on the disk.

The results for the other pins run against the TiNi-implanted disks shown in Table II were similar to those for the TiC pin just described. The TiC-Ni-Mo pin run against Si_3N_4 (couple 2), however, had a much higher nickel signal on the transfer layer, as well as having nickel on the unworn area. The transfer layer was much larger than even the other high μ_F pin (couple 3), and could account for some smearing of nickel onto the unworn areas. Since μ_F for this pin is the same as that for the TiC pin of couple 3, it is suspected that this difference could be related to slight variations in the orientation between the pin surfaces and the disks.

While little difference was found between the pin surfaces except as mentioned above, it appears that the pin composition could have played a role in the wear characteristics, although in a contradictory manner. The addition of nickel and molybdenum appeared to improve the wear characteristics of the partially stabilized zirconia - TiC couple, but not those of the Si_3N_4-TiC couple. Molybdenum was not detected on the surfaces of the TiC-Ni-Mo pins, however, probably due to its high volatility at the temperatures expected at the pin-disk interface. Since nickel transferred from the disk to the pins as shown for the case of the TiC pins, it also is not clear what role the addition of nickel to the pins played in the wear behavior.

2. Disks

The results of the analysis of the TiNi-implanted disks are shown in Figs. 18-25. Secondary electron micrographs and corresponding Auger elemental peak maps are given in Figs. 18-21, while typical Auger spectra and elemental depth profiles taken on, as well as distant from, the wear tracks are shown in Figs. 8-11. The results displayed in Figs. 4-7 were all taken at approximately the same sputter depth to facilitate comparison (sputter time $\tilde{=}$ 10-15 minutes including ~ 5-6 minutes to remove the silver coating). It was found during depth profiling that the implanted layers varied in thickness over the disk surfaces. Therefore,

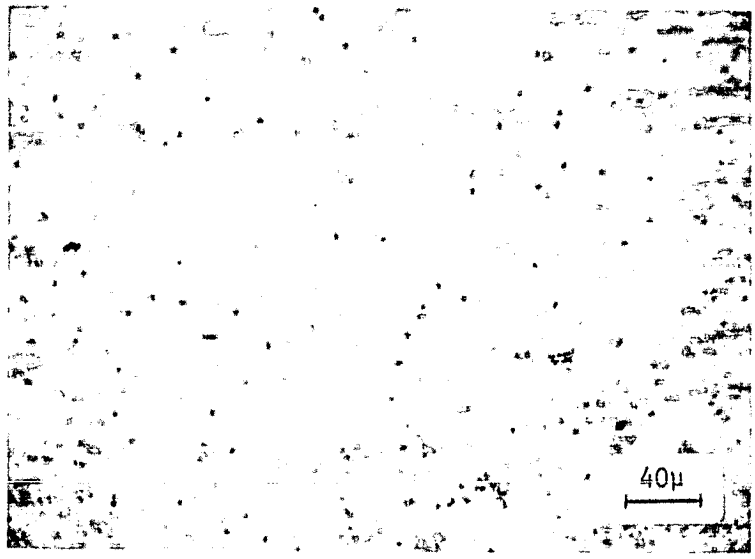

Figure 18. Wear Track of Si_3N_4 (Ti,Ni) Disk Run Against a TiC Pin (μ_F = 0.09) in a Diesel Environment at 800°C.

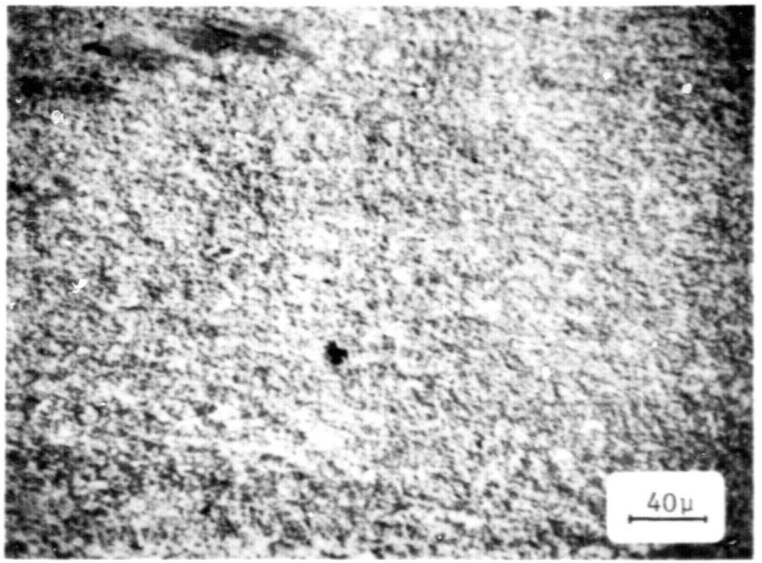

(a) SEM micrograph.

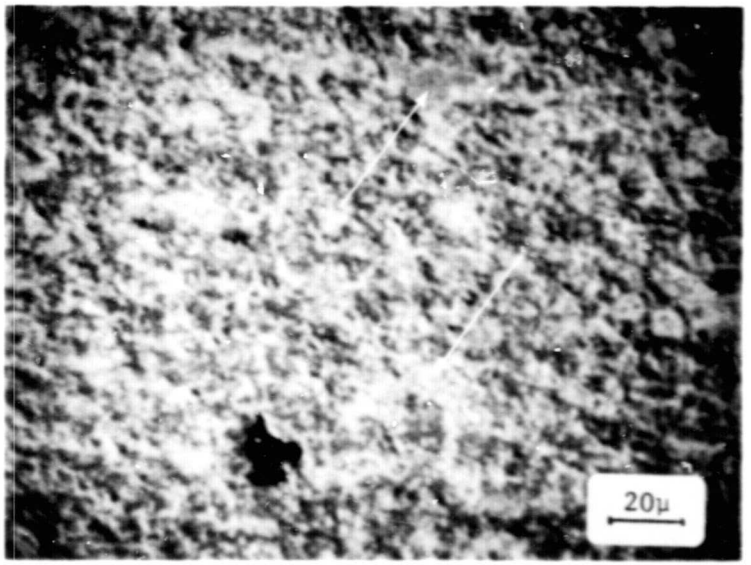

(b) SEM micrograph (see Figs. 19 c and d).

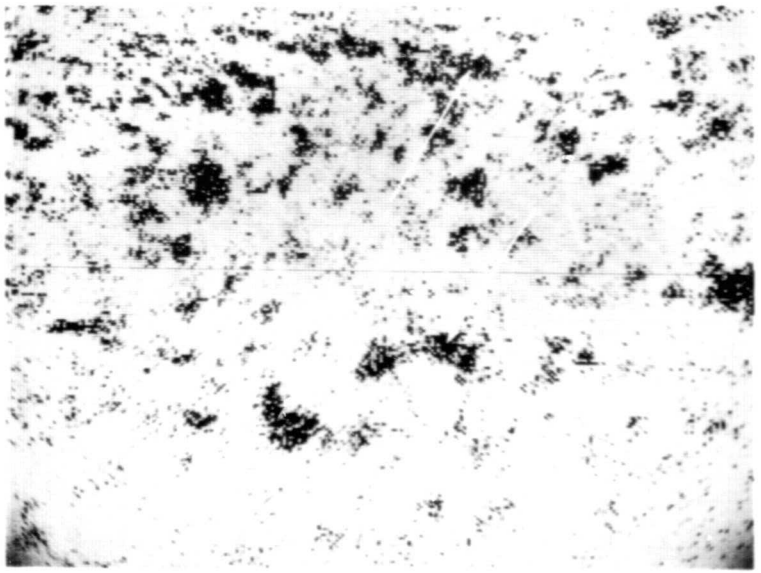

(c) Ti (387 eV) Auger map (see Fig. 19b).

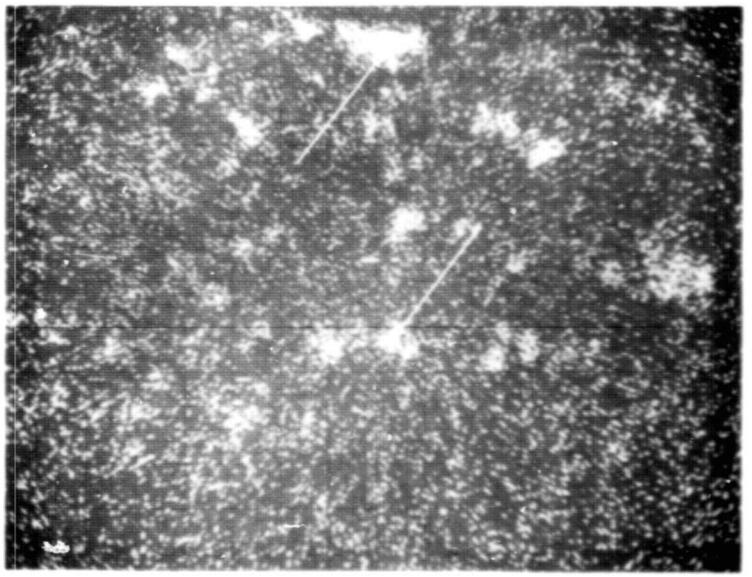

(d) Si (∿ 83 eV) Auger map (see Fig. 19b).

Figure 19. Wear Track of Si_3N_4 (Ti,Ni) Disk Run Against a TiC-Ni-Mo Pin (μ_F = 0.22) in a Diesel Environment at 800°C.

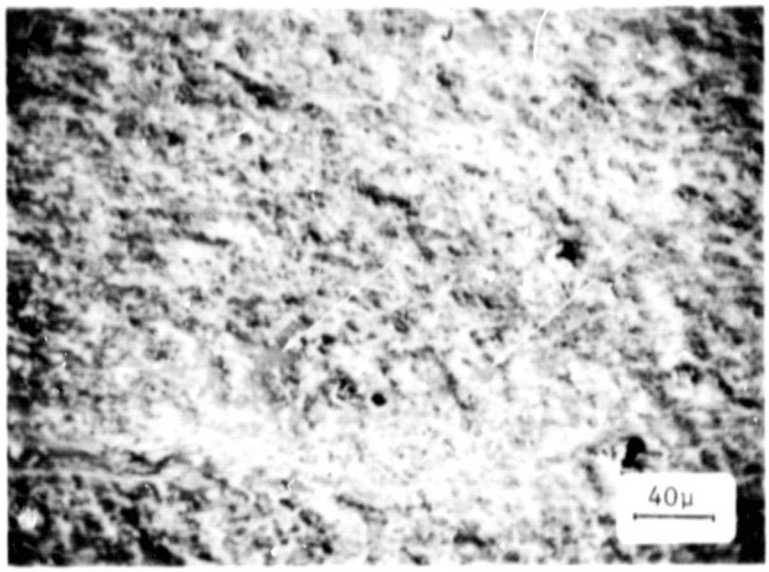

(a) SEM micrograph.

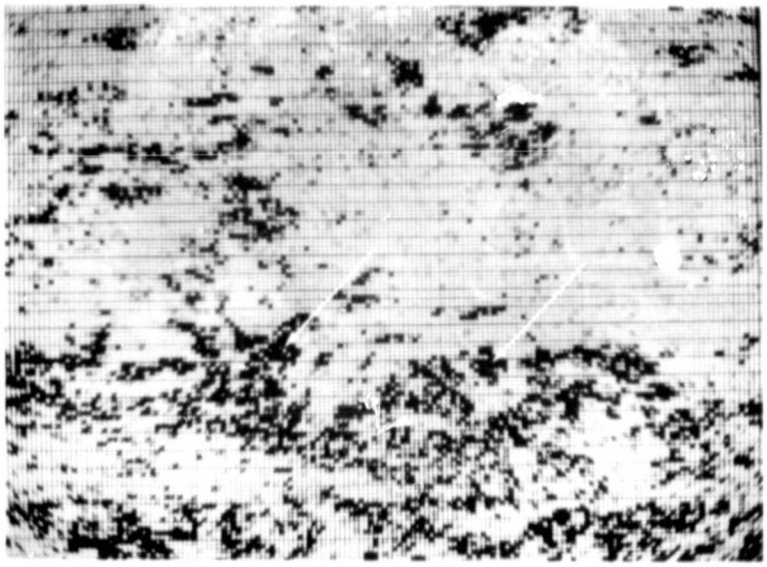

(b) Ti (387 eV) Auger map.

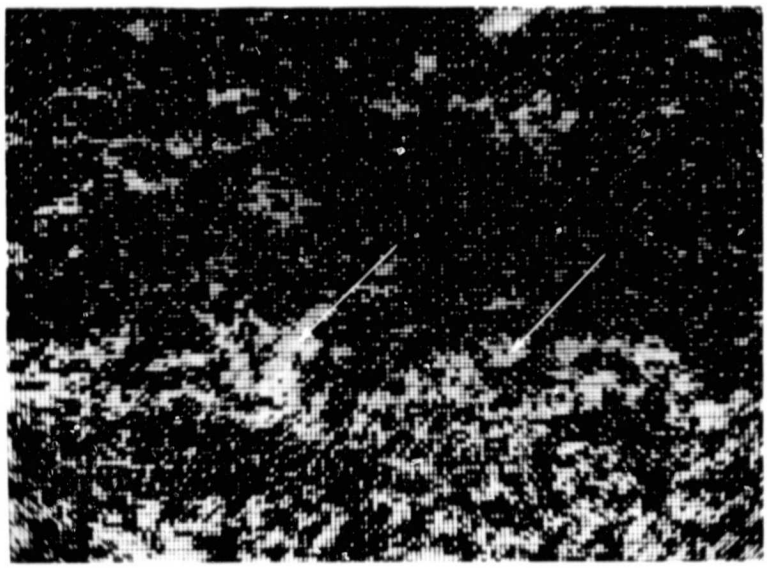

(c) Zr (147 eV) Auger map.

Figure 20. Wear Track of PSZ (Ti,Ni) Disk Run Against a TiC-Ni-Mo Pin (μ_F = 0.09) in a Diesel Environment at 800°C.

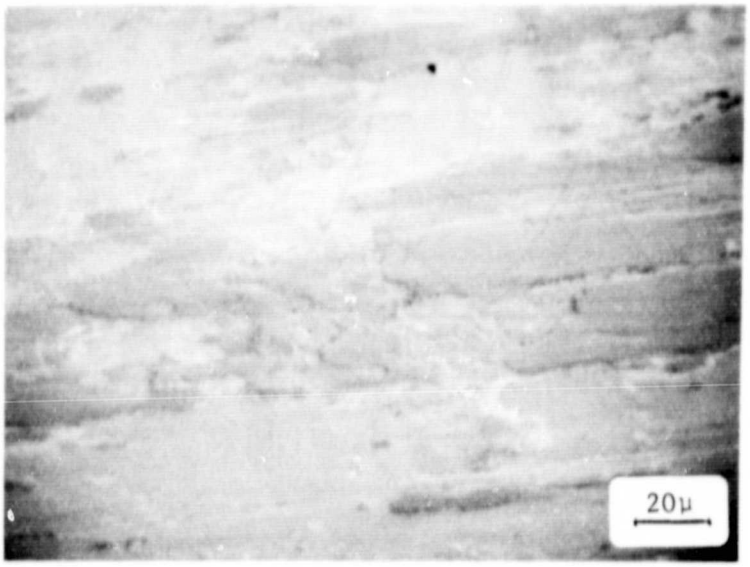

Figure 21. Wear Track of PSZ (Ti,Ni) Disk Run Against a TiC Pin (μ_F = 0.25) in a Diesel Environment at 800°C.

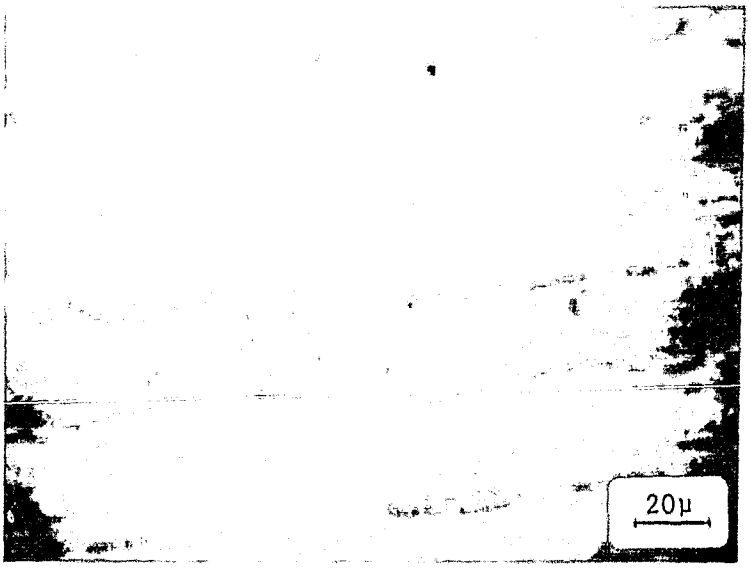

Figure 21. Wear Track of PSZ (Ti,Ni) Disk Run Against a TiC Pin (μ_F = 0.25) in a Diesel Environment at 800°C.

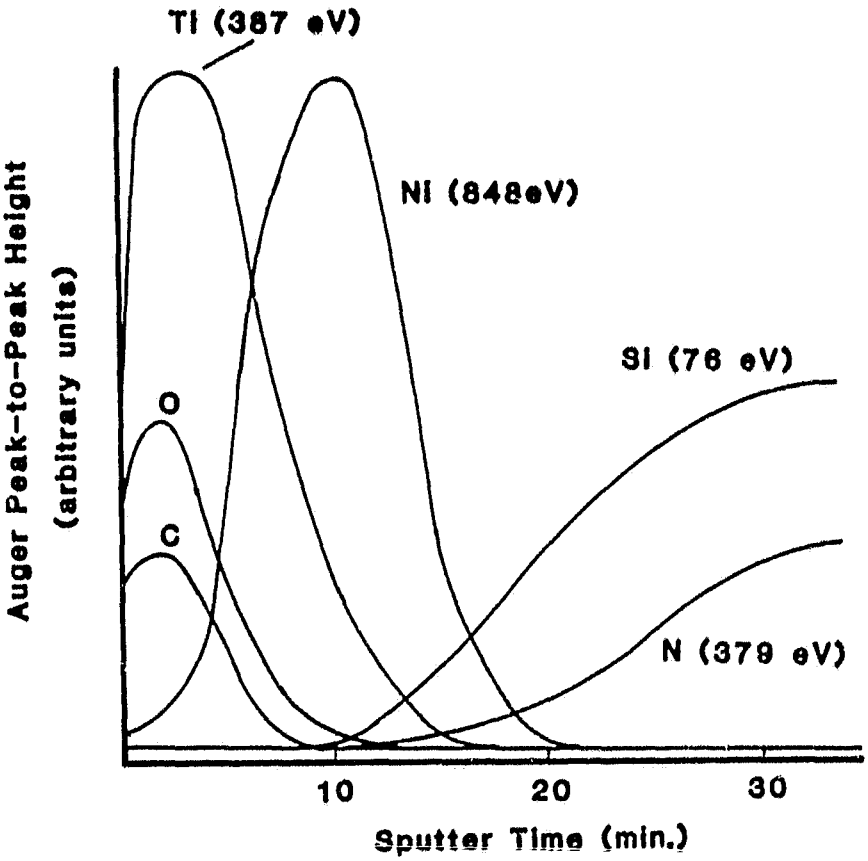

(a) Si_3N_4 (Ti,Ni).

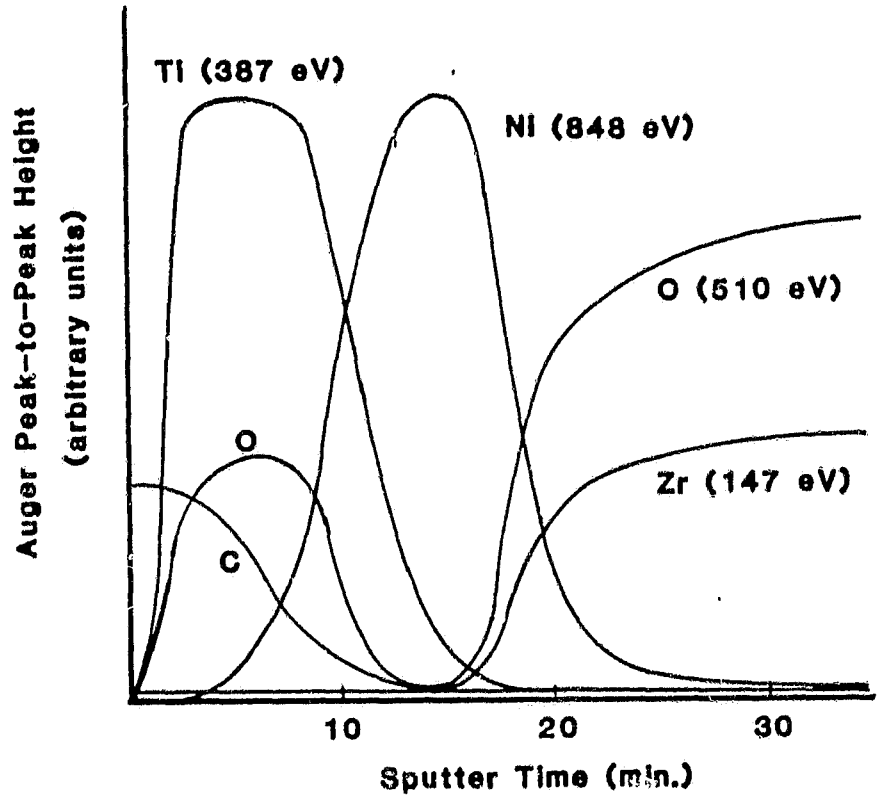

(b) Partially stabilized zirconia (Ti,Ni).

Figure 22. Elemental Depth Profiles of Ion-Implanted Disks Before Testing.

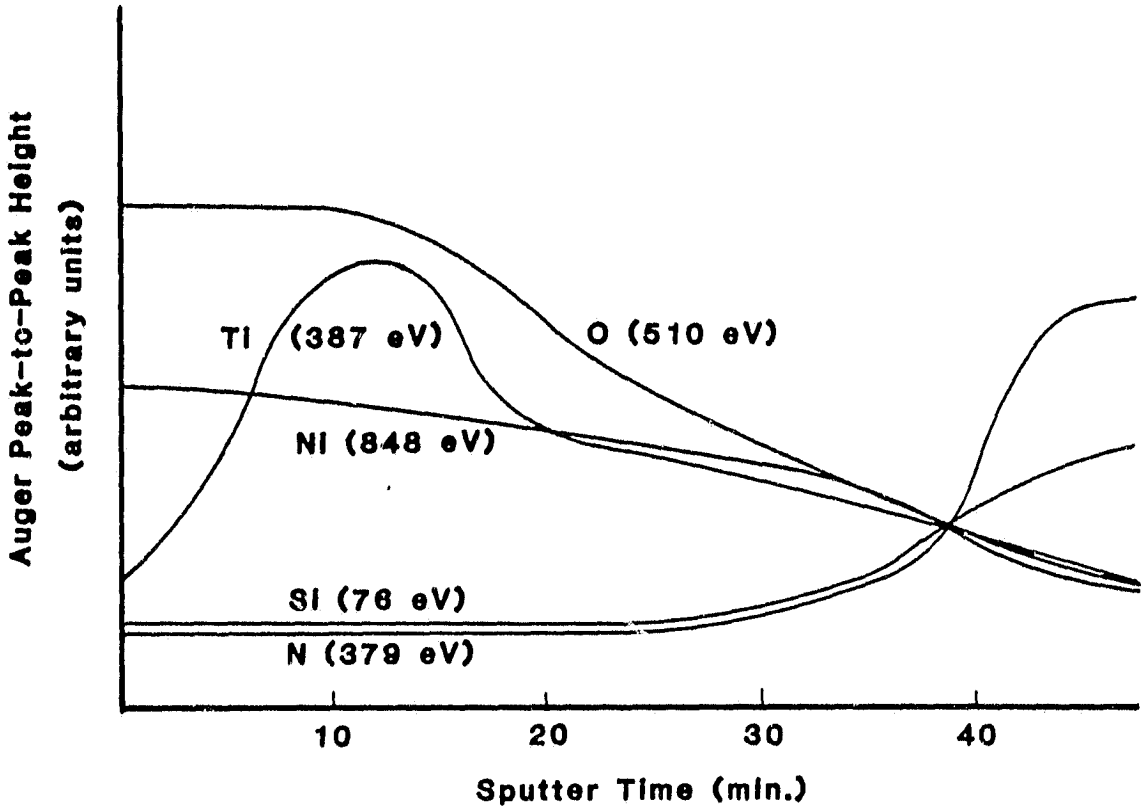

(a) Si_3N_4 (Ti,Ni).

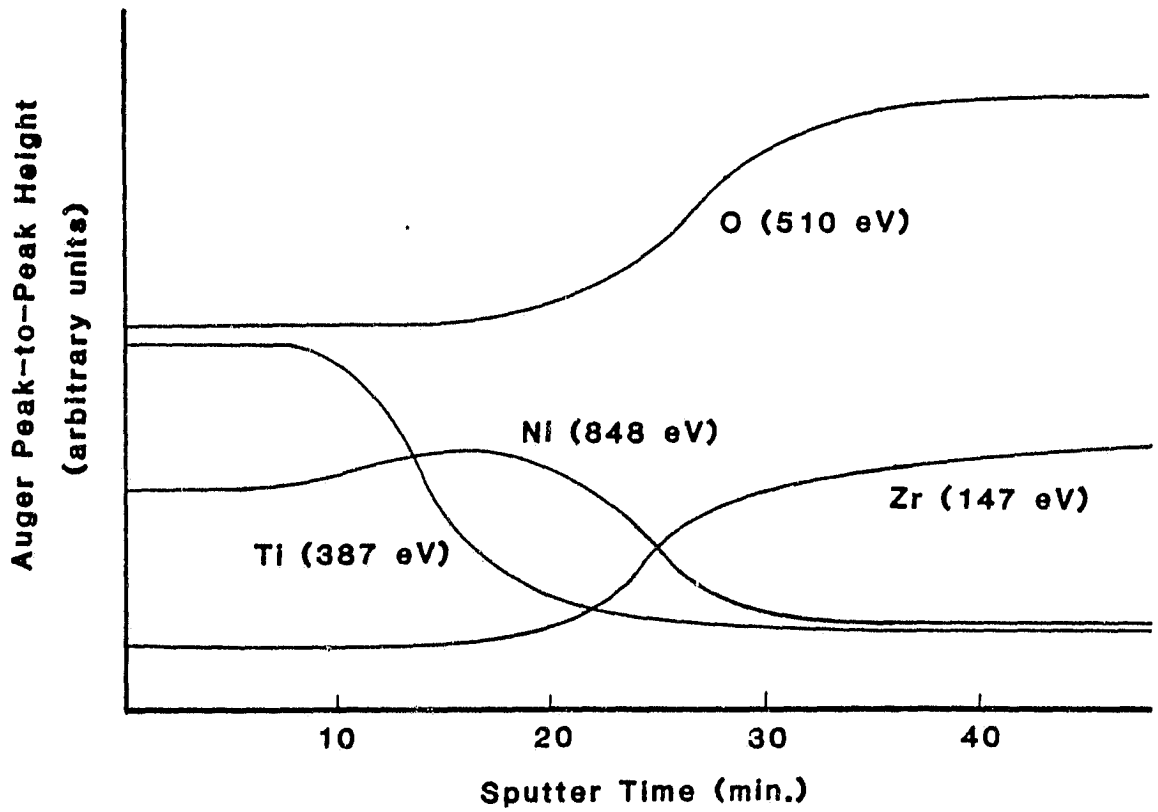

(b) Partially stabilized zirconia (Ti,Ni).

Figure 23. Elemental Depth Profiles Taken Away from the Wear Track.

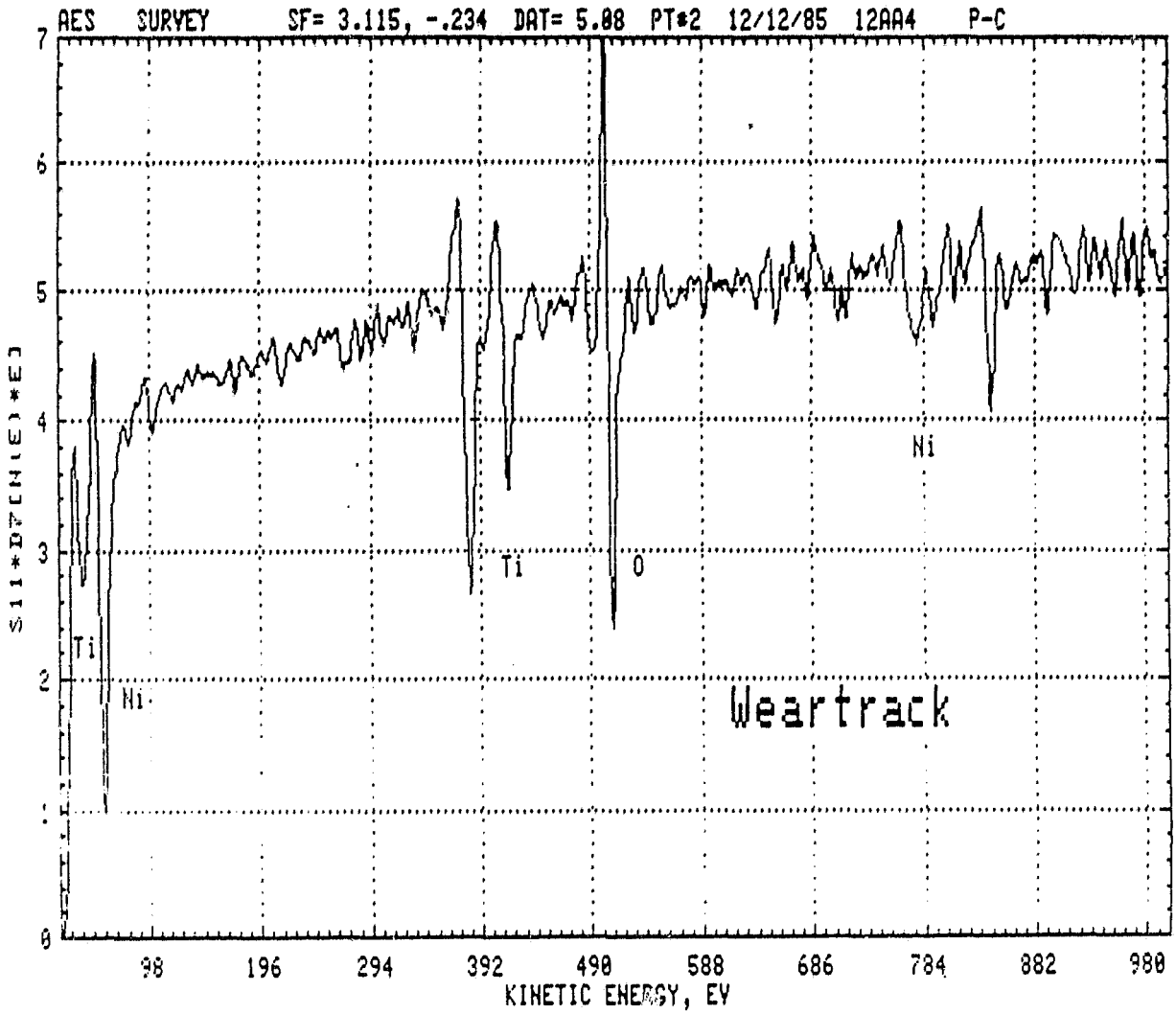

Figure 24. Typical Auger Spectrum Taken After Partial Sputter Removal of the Implanted (Ti,Ni) Layer from a Disk. Note the evidence for titanium oxide (40 eV peak, peak height rati $Ti_{387}/Ti_{418} > 1$).

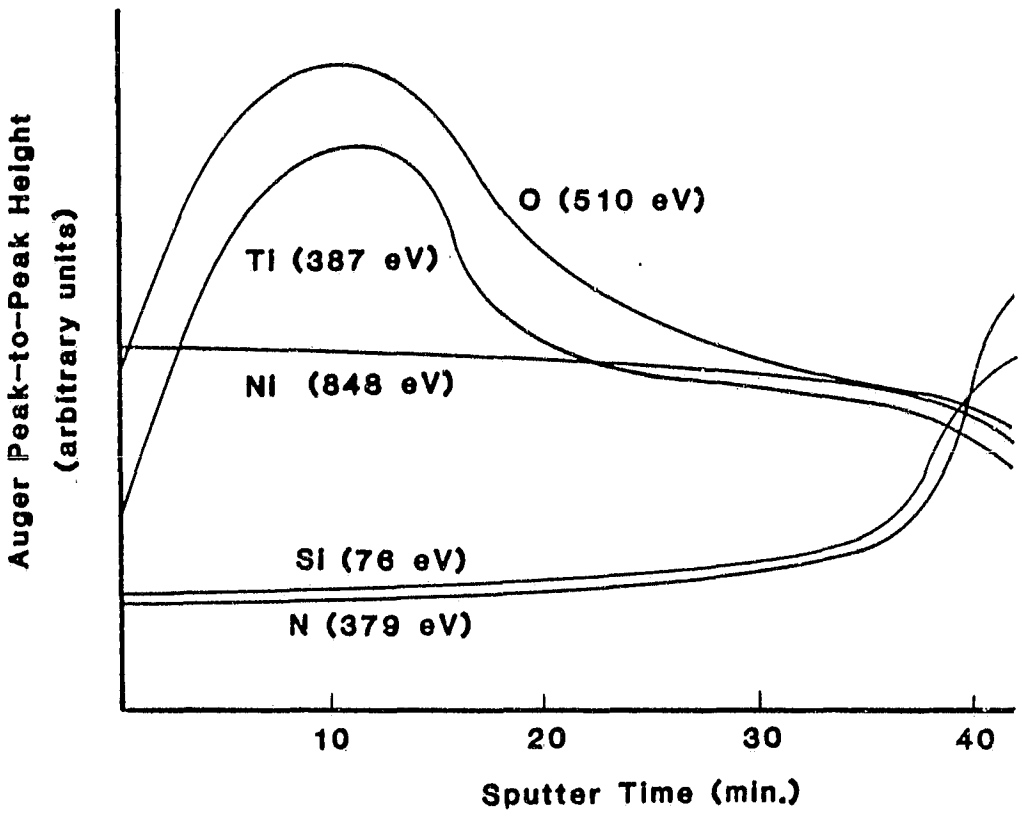

Figure 25. Elemental Depth Profile of an Implant Layer Laminate Left on the Wear Track of a Si_3N_4 Disk.

the profiles shown indicate the relative trends of elemental composition with depth, but no quantitative information is implied.

Elemental depth profiles of the disks as received after ion-implantation are shown in Fig. 22. The layer is clearly not homogeneously mixed, with the components lying more or less as they were put down--substrate, nickel, titanium. The titanium layer was probably slightly oxidized during implantation, and some carbon, probably from specimen handling, has also been implanted in the outer layer. As previously mentioned, this may account for some of the carbon found in the transfer layers on the pins.

The morphology of the wear tracks is shown in the secondary electron micrographs of Figs. 18-21. A comparison of Figs. 18 and 19a for Si_3N_4, and Figs. 20a and 21 for the zirconia, indicate that the wear tracks of the low μ_F disks have a finer structure than those of the corresponding high μ_F disks. The mechanism of wear appears to be that of delamination as first suggested by Suh (25), where material is removed in thin sheets by a shear-type deformation. The delamination generally occurs at the implanted layer-substrate interface, with the high μ_F disks showing a much larger degree of such delamination than the low μ_F disks. For the Si_3N_4 case, this can be seen in Figs. 19b-d, where the flat regions, examples of which are indicated by the arrows, correspond to regions of silicon and lack of the implant layer as seen in the Auger peak maps. The low μ_F Si_3N_4 disk also shows a delamination type of wear, seen by streaks of silver left where laminates have shadowed the neighboring region from the ion beam, Fig. 18, but little sign of the substrate was observed. Implant-substrate delamination is more obvious on the low μ_F zirconia disk, Fig. 20a-c, where arrows again indicate examples of where the substrate appears (Zr (147 eV) signal). The high μ_F zirconia disk, however, clearly shows the greater degree of delamination, Fig. 21, where the dark laminates consist of titanium and nickel, and the light areas are zirconium oxide.

While quantitative depth analysis of these specimens is made difficult due to surface roughness and composition induced preferential sputtering, elemental depth profiling has provided useful qualitative information about the chemistry of the observed wear tracks. Elemental depth profiles taken at various points on and away from the wear tracks indicate that, under the temperature and/or pin pressure conditions of the tests, the composition profile of the implant layer had changed considerably during the tests from that of the as-received disks, Fig. 22.

Typical depth profiles taken away from the wear track are shown in Fig. 23. In the case of the Si_3N_4 disks, Fig. 23a, it appears that the titanium layer has retained its profile while the nickel has diffused to the surface of the disk. While not obvious from the profiles themselves, examination of the individual spectra used to make up the silicon profiles indicate that silicon becomes detectable approximately halfway through the profile. The titanium profile has also been retained on the zirconia disk, Fig. 23b, but the layer is not as thick as that on

the Si_3N_4 disk, nor is nickel present on the surface. Zirconium was not detectable until near the end of the implanted layer. The implanted layer on both types of disks were clearly oxidized under the test conditions. The shape of the oxygen profile follows that of the titanium layer and changes in the titanium Auger spectra were similar to those observed for the pins, as shown in Fig. 24. This definitely does not, however, preclude the fact that the nickel layer may also be oxidized, since the nickel profile was flat.

Nickel tends to vaporize fairly easily at high temperature. A loss of nickel at the surface of the disks would thus not be unexpected. However, the presence of nickel on the surface of the Si_3N_4 disk, along with evidence of mixing of the substrate, indicates that the implanted layer may be better bound to Si_3N_4 than to zirconia. This could also be concluded from the SEM observations, where both the low and high μ_F zirconia disks exhibit more exposed substrate than the corresponding Si_3N_4 disks.

A typical elemental depth profile from the implanted layer left on the wear track is shown in Fig. 25. This example from a Si_3N_4 disk shows a small amount of nickel at the surface, followed by the titanium layer mixed with nickel. This is in contrast to the unworn areas which showed a thicker surface nickel layer as measured by sputter time. Slight variations in the thickness of the surface nickel layer on the wear tracks were noted depending on how high or low a particular lamination was situated relative to its surroundings. The laminates left on the zirconia disk wear tracks showed virtually no surface nickel. The pins run against them did, however, show a large amount of nickel. Analogous to the case of the unworn areas, it is possible that nickel diffused to the surface of the disks and then transferred to the pins. The fact that some nickel remained on the surface of the Si_3N_4 disks and not the zirconia disks, again indicates that the implant layer may be better bonded to Si_3N_4.

The thickness of the laminates could not be determined because of surface roughness effects on sputtering. Low regions, especially any exposed substrate, tended to be preferentially sputtered, making the laminates appear very thick. Assuming that nickel was removed from the surface (and possibly deposited on the pins), it would be logical to assume that the laminates would be thinner than the original implant layer. It is also possible, however, that material could have piled up locally on the wear track. The pin would then be riding on this raised lamination layer. This does not seem as likely, since a pileup would be indicated by a significant compositional change in the depth profiles, rather than just the removal of surface nickel.

Further evidence for the better mixing of the implant layer on Si_3N_4 rather than zirconia was obtained from analysis of the delaminated regions of the wear track. A thin layer of nickel generally covered these regions, although the substrate signal appeared fairly strong. Upon sputtering however, the nickel signal disappeared fairly rapidly from the zirconia disks, while it remained for some time on the Si_3N_4 disks.

C. Results of Analyses on Cobalt-Implanted and Nickel-Implated Disks

The results of the tests on cobalt implanted disks showed behavior in some ways similar to the titanium-nickel implanted disks. The cobalt implanted zirconia disks showed a low coefficient of friction when run against the TiC-Ni-Mo pin, and a much higher value when run against the TiC pin. However, unlike the titanium-nickel case, the Si_3N_4 disks showed no improvement when ion-implanted with cobalt.

Auger analysis of the cobalt implanted zirconia disks and the corresponding pins indicates that cobalt transfers from the disk surface to the pins. Elemental depth profiles indicate that both the pin and the disk cobalt layers are oxidized, implying the presence of a lubricating cobalt oxide film analogous to the titanium-nickel case. Disturbing, however, are the physical characteristics of the wear tracks, especially for the low coefficient of friction disk. Both wear tracks showed delamination of the cobalt layer, leaving exposed substrate. The wear track of the low coefficient of friction disk varied in width and amount of wear, ranging from the width of the pin and wear as heavy as that visible on the other three disks, to areas where the wear track is practically nonexistent. It is thus possible that the zirconia/TiC-Ni-Mo results were influencd by the alignment of the pins and disk. In any case, the cobalt results indicate the transfer and possible lubricating effect of a cobalt oxide layer.

The surface of the TiC-Ni-Mo pin also showed the strong presence of nickel. This indicates that nickel segregates to the pin surface, and may play a role in the friction and wear behavior of the ceramic couples. This also implies that nickel may have segregated from the pins in the case of the TiNi-implant tests, but would not be observable due to the nickel component of the implanted layer.

The results of the titanium-nickel and the cobalt implanted disks indicate that nickel may play a role in the friction and wear behavior of ion-implanted ceramics, either as a part of the implanted layer, or due to its presence in the pins. Therefore two Si_3N_4 disks were ion-implanted with a layer of nickel, and tested in diesel environment at 800°C and at room temperature.

The results of the friction and wear tests indicated that nickel improved the coefficient of friction of Si_3N_4, but not to the degree as that of the titanium-nickel implants, or the cobalt in zirconia implant. Analysis of the wear surfaces of the disks and the pins showed that the nickel layer was completely worn off the disk, and that no nickel transferred to the pins. The wear track showed cracking, especially near the edge of the crack, typical of the wear tracks of unmodified ceramics. The pin surfaces showed clear signs of wear, as opposed to the adherence of a transfer layer seen in the case of titanium-nickel and cobalt. Examination of the unworn areas after testing showed, however, that the nickel layer was much better mixed into the substrate than in the two previous cases.

D. Discussion

The results of this surface investigation into the wear of ion-implanted ceramic disks indicate that several factors may govern the wear properties of these materials in the high temperature environment used. These include the adhesion of the implanted layer to the ceramic, the transfer of material between the surfaces of the pins and disks, and the chemical state of the disk surface material (oxide) and the pin material.

The adhesion at the implant layer-ceramic boundary is clearly important in a delamination type of wear, since this would be the weakest interface. Both the micrographs and depth profiles indicate that for the TiNi-implanted disks, the TiNi layer adhered better to the Si_3N_4 than the zirconia in the low as well as the high μ_F cases. However, even on the low μ_F Si_3N_4 disk, small amounts of relatively bare substrate were occasionally detected, thus raising the possibility that a longer term test might result in the eventual removal of the implanted layer on all of the disks. The wear resistance of the layer on Si_3N_4 would then be of only temporary benefit. The cobalt and nickel layers did not appear to be bound as well to their respective substrates. It may be noted here that chromium implantation produced no beneficial effects in either disk material. On the contrary, it was almost completely worn off, leaving virtually no trace on the wear track, thus indicating poor adhesion to the substrate.

The transfer of material, or the formation of a surface oxide has been shown to be beneficial to the wear characteristics of many systems (40-41). In the present case, nickel appears to have been transferred from the disks to the pins, or vice versa as indicated by the results obtained from the pins run against the Co-implanted disks. Although it is highly likely that titanium transferred to the pins, it was not possible to determine definitely whether or not this was the case; a radioactive tracer technique would be useful in the case of either nickel or titanium. There is no doubt that the titanium present in both the pins and the implant layer has been oxidized. It is not clear whether one, or both, processes, nickel transfer and/or implant layer oxidation, are required to improve wear characteristics. Wear tests run at high temperatures in argon showed poorer wear characteristics than in the oxygen containing diesel environments, even though material transfer took place. However, as will be discussed shortly, TiC and TiC-Mo-Ni pins run against uncoated ceramic disks showed better wear characteristics than other pin materials, due to the transfer and oxidation of titanium from the pins to the disks.

Related to the material transfer question is the choice of pin material. For the present pin disk combinations involving the TiNi implant, the pin material played a confusing role. Nickel was clearly transferred to all four pins, but the two pin materials had opposite effects with respect to disk material in couples 1-4. On the other hand, nickel segregated from the TiC-Ni-Mo pins may have played a role in the case of the Co-implanted disks. This behavior is at the moment not understood. However, the choice of pin material has played a major role in other pin-disk

systems. TiC or TiC-Ni-Mo pins have produced lower coefficients of friction than silicon carbide pins when run against uncoated Si_3N_4 and zirconia, and chromium implanted Si_3N_4 and zirconia, disks. This probably is due to the fact that titanium transferred from the pins to the disks, while silicon did not (as observed using energy dispersive spectroscopy, EDS).

The results of the tests conducted on disks implanted only with nickel indicate that while nickel alone does not improve the friction and wear behavior of ceramics as well as other implant species, it may help provide better bonding of those species and/or their lubricating oxides. In the case of the titanium-nickel implants, titanium oxide appears to be responsible for the improved friction and wear behavior, but the nickel layer appears to be the bonding species which mixes into the substrate, especially in the case of Si_3N_4. In the case of the cobalt implant, segregation of nickel from the TiC-Ni-Mo pin may be responsible for the transferred cobalt adhering to the pin surface at least temporarily, thus delaying the degradation of the friction and wear properties due to the removal of the cobalt layer from the disk surface. Further work is required to determine the influence of nickel on the bonding and/or friction and wear behavior of ion-implanted ceramics. Also of interest would be to determine those species which can be coupled with nickel in an implant layer to provide those beneficial results. For example, the implantation of chromium alone apparently had no beneficial influence on the friction and wear behavior of either Si_3N_4 or zirconia, even when run against TiC-Ni-Mo pins. Chromium ion-mixed with nickel might do much better.

E. Conclusions

Surface studies have been performed with scanning Auger electron microscopy to examine the wear of ceramic materials to be used in high temperature adiabatic engines. The wear surfaces of pin-disk combinations showing promising wear properties in terms of low coefficients of friction and weight loss were examined and compared with those showing less promising wear properties. Of all pin-disk combinations tested, TiC or TiC-Ni-Mo pins run against Si_3N_4 or zirconia disks implanted with a double layer of titanium and nickel showed the best wear properties. There were significant differences among all of the combinations examined, however, which indicate that several factors play an important role in the wear process. These include:

- the transfer of material between members of a wear couple
- the formation of a possibly lubricating oxide layer
- the choice of pin material
- in the case of the surface treatment of ceramic wear parts such as with ion implantation, the adhesion properties of the surface layer.

F. Acknowledgement

The authors would like to acknowledge the capable assistance of Mr. A. Nicholls during the friction and wear testing. Helpful discussions with Dr. R. Kossowsky of Pennsylvania State University are greatly appreciated.

III. REFERENCES

1. J. Breznak, E. Breval, and N. H. MacMillan, Jour. Mat. Sci. 20: 4657 (1985).

2. T. Shimauchi, T. Murakami, T. Nakagaki, Y. Tsuya, and K. Umeda, Adiabatic Engines: Worldwide Review SP-571, Society of Automotive Engineers, Warrendale, PA, 21 (1984).

3. D. J. Boes, Proceedings 22nd CCM, Society of Automotive Engineers, Warrendale, PA, 323 (1984).

4. E. Rabinowicz, Friction and Wear of Materials, Wiley, NY, (1965).

5. K. Miyoshi and D. H. Buckley, in Tribology in the '80s 1: NASA CP-2300, NASA, Washington, DC, 291 (1984).

6. O. O. Adewoye and T. F. Page, Wear 70: 37 (1981).

7. D. W. Richerson, L. J. Lindberg, W. D. Carruthers and J. Dahn, Ceram. Eng. Sci. Proc. 2: 578 (1981).

8. J. R. Smyth and D. W. Richerson, Ceram. Eng. Sci. Proc. 4: 663 (1983).

9. M. B. Peterson and S. F. Murray, Metals Eng. Quart. 7(2): 22 (1967).

10. A. F. McLean, Amer. Ceram. Soc. Bull. 61: 861 (1982).

11. D. Tabor, J. Lubrication Technol. 130: 169 (1981).

12. R. P. Steijn, Wear 7: 48-66 (1964).

13. Donald H. Buckley, Ceramic Bulletin 51: 884-905 (1972).

14. D. J. Barnes and B. D. Powell, Wear 32: 195-202 (1975).

15. H. Shimura and Y. Tsuya, Proc. Int. Conf. Wear of Mats., St. Louis, April 1977, ASME, NY, 452 (1977).

16. M. Hirano and S. Miyake, Jour. Tribology 107: 467 (1985).

17. J. K. Lancaster, Jour. Tribology 107: 437 (1985).

18. E. F. Finkin, S. J. Calabrese, M. B. Peterson, ASLE Preprint No. 72LC-7C-2 (1972).

19. L. B. Sibley and C. M. Allen, Wear 5: 312-329 (1962).

20. Advanced Mechanical Technology, Inc., "Evaluation of Improved Materials for Stationary Diesel Engines Operating on Residual and Coal Based Fuels", U. S. Department of Energy Contract No. DE-AC-03-79ET15444 (1980).

21. S. Gray, Adiabatic Engines: Worldwide Review SP-571, Society of Automotive Engineers, Warrendale, PA, 21 (1984).

22. W. J. Lackey and D. P. Stinton, Proceedings 22nd CCM, Society of Automotive Engineers, Warrendale, PA, 445 (1984).

23. S. Jahanmir, N. P. Suh, and E. P. Abrahamson, Wear 28: 235 (1974).

24. H.-C. Sin and N. P. Suh, J. App. Mech. 51: 317 (1984).

25. N. P. Suh, Wear 25: 111 (1973).

26. Y. Yamamoto and D. H. Buckley, ASLE Trans. 26: 277 (1982).

27. B. Carriere, et al, Vacuum 22(10): 485-487 (1972).

28. B. Carriere and B. Lang, Surf. Sci. 64: 209-223 (1977).

29. F. Fransen, et al, Surf. and Interface Anal. 7(2): 79-87 (1985).

30. O. C. Wells, et al, in Scanning Electron Microscopy, McGraw-Hill Book Co., NY, 150-156 (1974).

31. H. L. Marcus, et al, in Fracture Mechanics of Ceramics Vol. 1 Concepts, Flaws and Fractography, R. C. Bradt et al, eds., Plenum Press, NY, 387-398 (1974).

32. C. G. Pantano and T. E. Madey, Appl. of Surf. Sci. 7: 115-141 (1981).

33. H. Viefhaus, Private Communication.

34. S. Hofmann in Practical Surface Analysis by Auger and X-Ray Photoelectron Spectroscopy, D. Briggs and M. P. Seah, eds., John Wiley and Sons, Chichester, U.K., Ch. 4, 141-180 (1983).

35. H. E. Bishop, et al, Surf. Sci. 24: 1-17 (1971).

36. M. C. Burrell and N. R. Armstrong, J. Vac. Sci. Tech. A 1(4): 1831-1836 (1983).

37. L. E. Davis, et al, editors, Handbook of Auger Electron Spectroscopy, 2nd Edition, Perkin-Elmer Corp., Eden Prairie, Minn., (1978).

38. P. H. McBreen and M. Polak, Surf. Sci. 163: L666-L674 (1985).

39. P. H. Holloway and R. A. Outlaw, Surf. Sci. 111: 300-316 (1981).

40. D. H. Buckley, Surface Effects in Adhesion, Friction, Wear, and Lubrication, Tribology Series, 5, Elsevier Scientific Pub. Co., Amsterdam, (1984).

41. I. L. Singer, Appl. of Surf. Science 18: 28-62 (1984).